

Predicting the susceptibility to gully initiation in data-poor regions



Olivier Dewitte^{a,b,c,*}, Mohamed Daoudi^d, Claudio Bosco^e, Miet Van Den Eeckhaut^b

^a Royal Museum for Central Africa, Department of Earth Sciences, Tervuren, Belgium

^b European Commission, Joint Research Centre, Institute for Environment and Sustainability, Ispra, Italy

^c Ghent University, Department of Geology and Soil Science, Ghent, Belgium

^d King Abdulaziz University, Department of Geography and Geographic Information Systems, Jeddah, Kingdom of Saudi Arabia

^e Loughborough University, School of Civil and Building Engineering, Loughborough, United Kingdom

ARTICLE INFO

Article history:

Received 14 March 2013

Received in revised form 15 July 2014

Accepted 9 August 2014

Available online 10 September 2014

Keywords:

Gully erosion

Susceptibility modelling

Slope–area thresholds

Logistic regression analysis

Initiation area

ABSTRACT

Permanent gullies are common features in many landscapes and quite often they represent the dominant soil erosion process. Once a gully has initiated, field evidence shows that gully channel formation and headcut migration rapidly occur. In order to prevent the undesired effects of gully erosion, there is a need to predict the places where new gullies might initiate. From detailed field measurements, studies have demonstrated strong inverse relationships between slope gradient of the soil surface (S) and drainage area (A) at the point of channel initiation across catchments in different climatic and morphological environments. Such slope–area thresholds (S – A) can be used to predict locations in the landscape where gullies might initiate. However, acquiring S – A requires detailed field investigations and accurate high resolution digital elevation data, which are usually difficult to acquire. To circumvent this issue, we propose a two-step method that uses published S – A thresholds and a logistic regression analysis (LR). S – A thresholds from the literature are used as proxies of field measurement. The method is calibrated and validated on a watershed, close to the town of Algiers, northern Algeria, where gully erosion affects most of the slopes. The gullies extend up to several kilometres in length and cover 16% of the study area. First we reconstruct the initiation areas of the existing gullies by applying S – A thresholds for similar environments. Then, using the initiation area map as the dependent variable with combinations of topographic and lithological predictor variables, we calibrate several LR models. It provides relevant results in terms of statistical reliability, prediction performance, and geomorphological significance. This method using S – A thresholds with data-driven assessment methods like LR proves to be efficient when applied to common spatial data and establishes a methodology that will allow similar studies to be undertaken elsewhere.

© 2014 Elsevier B.V. All rights reserved.

1. Introduction

Permanent gullies, i.e. gullies that cannot be obliterated by ploughing, are common features in many landscapes and often, like in Mediterranean and arid environments, they represent the dominant process of soil erosion by water (Vandekerckhove et al., 2000; Poesen et al., 2002, 2003). Gully erosion is responsible for soil degradation, increase in sediment delivery, and reduction of water quality. It is also responsible for a decreased water travel time to rivers (and hence increased flooding probabilities), for the filling up of ponds and reservoirs, and for the destruction of buildings, fences, and roads. Gully erosion is highly sensitive to climate and land use changes (Poesen et al., 2002, 2003).

The initiation and the growth of a gully and gully system is complex (Istanbulluoglu et al., 2002). From field evidence, it is known that gully channel formation and headcut migration are usually very rapid following the initiation of the gully (e.g., Rutherford et al., 1997; Sidorchuk,

1999; Nachtergaele et al., 2002; Nyssen et al., 2006; Gómez Gutiérrez et al., 2009a; Seeger et al., 2009). In order to prevent the undesired effects of gullies, there is a need to anticipate the places where new gullies might initiate.

To predict where gully erosion will occur in the landscape by the extension of an existing gully or the formation of a new gully is difficult (Bull and Kirkby, 1997; Poesen et al., 2003, 2011). Gully initiation clearly is controlled by a variety of environmental conditions that can be modelled as threshold phenomena. Montgomery and Dietrich (1988, 1989, 1992, 1994) and Dietrich et al. (1992, 1993) were among the first authors to explore topographic thresholds on the occurrence of erosion channels. From detailed field measurements and the use of high-resolution digital terrain models (DTMs), they found a strong inverse relationships between slope gradient of the soil surface at the point of gully initiation (S) and contributing drainage area (A , proportional to runoff discharge) for a given environmental condition. The topographic threshold is based on the assumption that in a landscape with a given climate, pedology, lithology, and vegetation, for a given S , there exists a critical A necessary to produce sufficient runoff for gully initiation (Montgomery and Dietrich, 1988, 1989). For different environmental

* Corresponding author at: Royal Museum For Central Africa, Department of Earth Sciences, Tervuren, Belgium. Tel.: +32 27695452.

E-mail address: olivier.dewitte@africamuseum.be (O. Dewitte).

conditions and different gully initiating processes (e.g. Horton overland flow, saturation overland flow, and shallow small landsliding) different topographic thresholds apply (Montgomery and Dietrich, 1988; Dietrich et al., 1992; Montgomery and Dietrich, 1994). Such slope-area thresholds ($S-A$) are therefore a useful predictor to forecast the location in the landscape where gullies might initiate (Montgomery and Dietrich, 1992; Dietrich et al., 1993).

Other attempts to map susceptibility to gully initiation through the use of $S-A$ relationships have been carried out (e.g., Prosser and Abernethy, 1996; Vandaele et al., 1996; Desmet et al., 1999; Vandekerckhove et al., 2000; Istanbuluoglu et al., 2002; Kirkby et al., 2003; Morgan and Mngomezulu, 2003; Vanwallegem et al., 2003; Hancock and Evans, 2006; Jetten et al., 2006; Pederson et al., 2006; Lesschen et al., 2007; Svoray and Markovitch, 2009; Millares et al., 2012). Although some of these studies were capable of predicting gully location, they require detailed field measurements and high resolution digital elevation data as input; which is in most cases difficult to acquire.

Data-driven assessment methods have also been applied to predict landscape susceptibility to gully erosion. In these methods combinations of environmental factors controlling the occurrence of the existing gullies are statistically evaluated, and quantitative predictions are made for current non-gully-affected areas with similar environmental conditions (e.g. Meyer and Martinez-Casasnovas, 1999; Hughes et al., 2001; Bou Kheir et al., 2007; Geissen et al., 2007; Vanwallegem et al., 2008; Gómez Gutiérrez et al., 2009b,c; Ndomba et al., 2009; Pike et al., 2009; Kuhnert et al., 2010; Akgün and Türk, 2011; Conforti et al., 2011; Eustace et al., 2011; Luca et al., 2011; Märker et al., 2011; Svoray et al., 2012; Conoscenti et al., 2013). These models are simple in their concept, do not necessarily need to rely on in situ field measurements, and have proved to be capable of predicting gully location even when using predictor variables extracted from common spatial data that are readily available for data-poor regions (e.g. global satellite-derived elevation data, basic topographic and lithological maps, and aerial photographs). A main advantage of these models is that the amount of information they can consider through the use of a potentially large panel of environmental factors can be just as important as the information contained in S and A alone. However, the spatial resolution of these datasets is often relatively low considering the actual size of the gullies and, when field information is lacking, to distinguish between the gully initiation area and its extension is difficult (Vanwallegem et al., 2008; Svoray et al., 2012). So far, most of these studies applying data-driven methods did not make this distinction and failed at predicting the actual initiation area of the gullies.

The objective of our research is therefore to develop a quantitative method gathering the advantages of both the threshold and the data-driven approaches for allowing the susceptibility to gully initiation to be predicted with readily available common spatial data. Our attention will be focused on the original point of gully initiation, i.e. before erosion leads to development of the gully. We propose a two-step method that uses published data on $S-A$ thresholds and a logistic regression analysis (LR) (Fig. 1). LR is a multivariate statistical method widely used for the prediction of the spatial occurrence of surface processes such as mass movements (e.g. Dai et al., 2004; Van Den Eckhaut et al., 2006; Rossi et al., 2010; Guns and Vanacker, 2012; Bosco et al., 2013), and that has already proved its appropriateness for gully erosion (e.g., Meyer and Martinez-Casasnovas, 1999; Vanwallegem et al., 2008; Pike et al., 2009; Akgün and Türk, 2011; Luca et al., 2011; Svoray et al., 2012). LR is a low data demanding technique, requiring predictor variables easily extractable from common spatial data, and yields directly a probability of occurrence of the studied process (Hosmer and Lemeshow, 2000). Published $S-A$ thresholds are used as field measurement proxies.

2. Material

In order to facilitate the method's development and to focus on the $S-A$ thresholds, a region characterized by a complex topography with

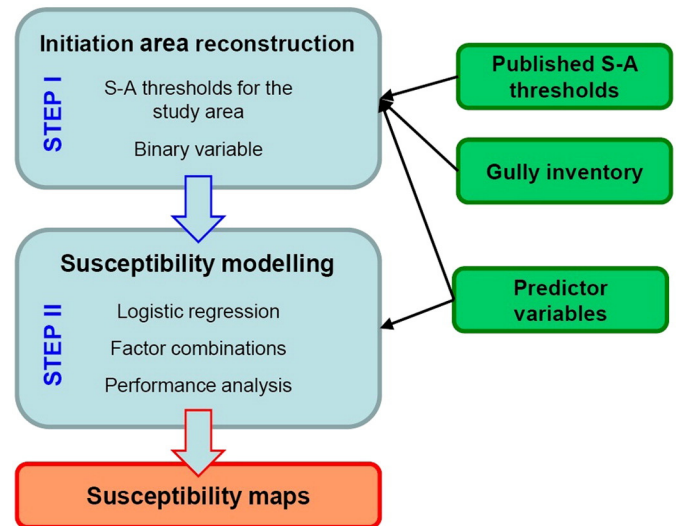


Fig. 1. General framework of the two-step method used to predict the susceptibility to gully initiation.

a wide range of slope configurations and where environmental conditions such as lithology and soils are favourable to gully development is selected.

2.1. Study area

We focus on a 51 km² sub-basin of the Isser River watershed in northern Algeria where the environmental conditions are favourable to gully development. The area is located approximately 80 km south east of Algiers in the Tell Atlas (Fig. 2). The climate is classified as Mediterranean close to semi-arid conditions, especially during the driest years. The average annual precipitation is approximately 400 mm. Precipitation is often caused by thunderstorms and is irregularly distributed throughout the year with a maximum in winter (70% of the precipitation between October and March) and a minimum in summer (Touazi et al., 2004).

The elevation of the sub-basin ranges from ~700 to ~1300 m above sea level. The lithology consists mainly of Paleocene–Eocene marls and calcareous marls (~70% of the total area), Cretaceous marls and limestones (~20%), and Quaternary alluvial deposits (~10%) (Fig. 2). These unconsolidated and poorly sorted materials are favourable conditions for gully development (Poesen et al., 2003). The majority of soils in this Mediterranean mountainous terrain are weakly developed Regosols formed on the unconsolidated marls (Daoudi, 2008). The pattern of vegetation and land use forms a mosaic of cultivated lands, rangelands, and scrublands; ninety-five percent of the zone having a sparse vegetation cover (Daoudi, 2008). The road network and building infrastructures are of limited extent.

Gully development is a widespread process in the watershed extending over most slopes (Fig. 2). Gully channels occupy 16% of the study area; which corresponds to a relatively high proportion compared to other watersheds in similar environments (Poesen et al., 2003). The permanent gullies vary in size and in shape. They can extend up to several kilometres in length and several tens of meters in width. In some cases their depth can be up to 10 m (Daoudi, 2008). Some gullies have a basic linear shape with one headcut linear gully (LG); the largest of them extending principally in the Eastern side of the watershed where the slope profiles tend to be more regular and the local relief is higher (Fig. 2C). Gullies develop also into complex gully systems (GS) that divide into several branches and multiple headcuts (Fig. 2B). Some of them have one or several bifurcations that arise either at the gully head or along the channel (Bull and Kirkby, 1997). Geomorphological evidence identifiable in aerial photographs of 1992 (Table 1) and

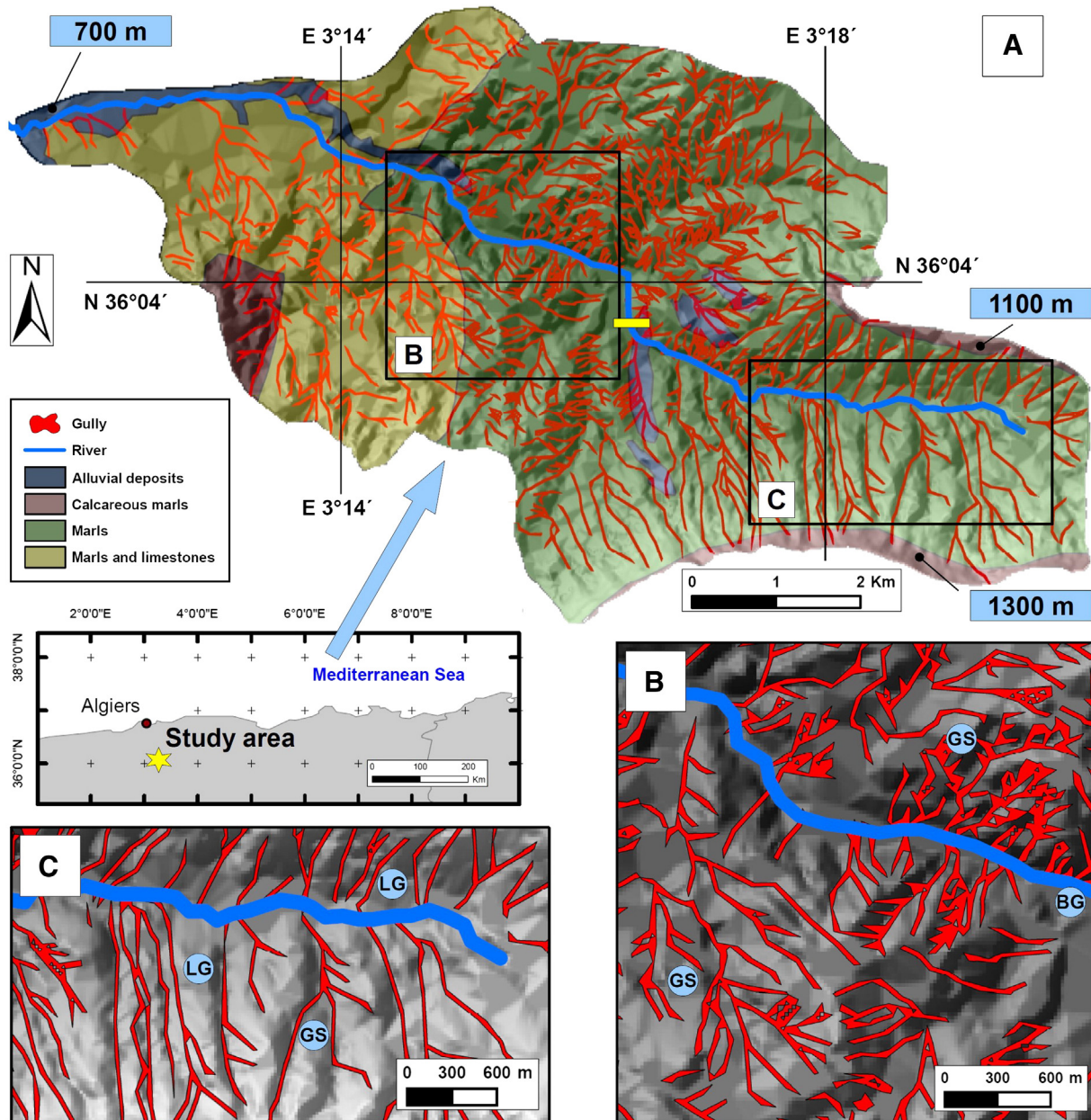


Fig. 2. Location of the study area (51 km²) in northern Algeria. (A) Watershed with gully distribution, lithological sketch, and relief. The yellow bar across the river shows a reservoir dam that was built after 1992. (B, C) Close-ups illustrating linear gullies (LG), complex gully systems (GS), and bank gullies (BG). Gully, lithology, and relief data are derived from the ancillary data described in Table 1.

2009 and 2012 Google Earth images, attest that soil erosion (and implicitly gully) is currently active in this area: fresh sediment accumulations in the river channel are visible as well as the filling up of a recently built reservoir (Fig. 2A) that does not appear in 1992. It is nevertheless impossible to infer about the current stage at which the gullies

are in their erosion cycle (active or stable). The linear gullies that extend perpendicularly from both the north-east and south-east ridges in the steepest parts of the watershed (Fig. 2C) are evenly spaced, suggesting an example of self-organization in the landscape due to the uniform properties of the lithology (Perron et al., 2009).

Table 1

Ancillary spatial data used for the modelling.

Type	Scale	Date	Source
Aerial photographs	~1:40 000	1992	Institut National de Cartographie et de Télédétection – Algeria
Topographic map	1:50 000*	1960**	Institut Géographique National de France (Feuille 111 – Souagui)
Lithological map	1:50 000	1961	Service de la Carte Géologique d’Algérie

* Contour interval is 20 m.

** Compiled from aerial photographs taken in 1953.

Concerning the processes at the origin of the gullies, it is verified in the field that the few landslides present in the area (not visible on the aerial photographs) are of very limited spatial extent and are not linked to the occurrence of the gullies (Daoudi, 2008), which supports hydraulic erosion as the dominant gully-initiating process and not mass movement (Montgomery and Dietrich, 1994). Some gullies are probably the result of several initiations occurring independently at a series of knickpoints along the slope profile and connected to each other while migrating (e.g., Pederson et al., 2006). Based on observations published in other studies, we can assume that the majority of the gullies are regressive and expanded by headcut migration (Poesen et al., 2002)

Bank gullies (BG) should also be present in the watershed. Some of the tributary channels of the river could be assumed to have partly initiated as bank gullies, especially the short linear segments (Fig. 2B).

However, we do not know when the gullies initiated and what climatic conditions prevailed at that time. They might be the result of several initiation phases and cycles spanning an unknown period of time (Vanwallegem et al., 2005a; Pelletier et al., 2011; Dotterweich et al., 2012). While it is known that during the last centuries the climatic conditions of northern Algeria remained quite similar to the current ones, with a recent shift towards drier conditions over the region (Touchan et al., 2011), the vegetation cover and the land use characteristics might be affected by more significant changes.

Wildfires frequently happen in Mediterranean environments and their vegetation-induced changes can cause the occurrence of gullies (Shakesby and Doerr, 2006). Also, with regard to the current land use conditions in the watershed, it can be assumed that the initiation of some gullies is a consequence of human-induced vegetation changes and farming practice such as ploughing (maybe in combination with extreme weather conditions) (e.g., Poesen et al., 2003; Nyssen et al., 2006; Zucca et al., 2006; Vanwallegem et al., 2008; Frankl et al., 2011; Pelletier et al., 2011). Although of limited extent in the watershed, road construction may have also increased susceptibility to erosion (Montgomery, 1994; Nyssen et al., 2002; Takken et al., 2008; Makanzu Imwangana et al., 2014). Such assumptions about human impact give phases of gully initiation that can easily span several centuries (Poesen et al., 2003; Pelletier et al., 2011; Dotterweich et al., 2012).

2.2. Predictor variables

The ancillary spatial information available for the study area is shown in Table 1. Aerial photographs taken in 1992 were used to map the gullies presented in Fig. 2. The topographic and lithological maps were used for extracting the predictor variables, i.e. the environmental factors that are supposed to have a role in the occurrence of the gullies. The raster maps representing the predictor variables were resampled at the same grid size of 20 m; this resolution is a suitable value according to the scale of the topographic map (1:50,000), its contour interval (20 m) and the complexity of terrain (Hengl, 2006). This resolution can distinguish between gully initiation area and gully extension area (Fig. 3).

The predictor variables need to consider the prevailing environmental conditions before gullies initiated. Although, from a chronological perspective, the topographic data were derived from aerial photographs that had been taken almost 40 years before those used for mapping the gullies (respectively 1953 and 1992; see Table 1), it is certain that some of these gullies developed before 1953 and had already shaped the landscape. The development of gullies implies the presence of scarps delimiting the gully channels. However, at a scale of 1:50,000 and with a contour interval of 20 m, topographic variations such as those induced by these scarps cannot be represented on the map. Therefore the map gives a smoothed picture of the actual soil surface morphology, so that it is a realistic assumption that the 20-m resolution DTM we used to derive the predictor variables corresponds to the pre-erosion topographic conditions without gully scarp.

Nine potential predictor variables used as independent variables in the modelling were extracted from the 20 m resolution DTM with ArcGIS software:

- Primary topographic attributes: elevation (m), slope angle (degrees), slope aspect (degrees clockwise from north), profile curvature ($\times 10^{-2} \text{ m}^{-1}$), planform curvature ($\times 10^{-2} \text{ m}^{-1}$), and contributing drainage area (pixel);
- Secondary topographic attributes: Sediment Transport Capacity Index (*TCI*), Stream Power Index (*SPI*), and Topographic Wetness Index (*TWI*).

The attributes “elevation” and “slope aspect” are considered as factors reflecting the climatic conditions (spatial variation of precipitation, temperature, and solar irradiation). The other primary attributes are taken for their potential influence on the superficial water runoff (overland flow). Contributing drainage area was derived from the hydrologically corrected DTM.

The three secondary attributes are hydrologically-based compound indices with the potential to predict the spatial distribution of soil properties having an impact on soil erosion (e.g., Daba et al., 2003; Nefeslioglu et al., 2008; Kakembo et al., 2009; Pike et al., 2009; Hancock and Evans, 2010; Conforti et al., 2011; Conoscenti et al., 2013).

TCI has been used to characterize erosion and deposition processes and, in particular, the effect of topography on soil erosion by water (Nefeslioglu et al., 2008; Pike et al., 2009; Conforti et al., 2011; Conoscenti et al., 2013). *TCI* based on the stream power theory is analogous to the slope length and steepness factor (*LS*) in the universal soil loss equation (USLE; Wischmeier and Smith, 1978), but is applicable to three-dimensional landscapes (Moore and Burch, 1986; Moore et al., 1991, 1993). It (TCI_M) can be expressed as:

$$TCI_M = LS = (A_s/a_0)^m (\sin\theta/b_0)^n \quad (1)$$

where A_s is the specific catchment area or unit contributing area ($\text{m}^2 \text{ m}^{-1}$) defined as the upslope area draining across a unit width of contour, θ is the slope angle (degrees), $a_0 = 22.13 \text{ m}$ is the standard USLE plot length, $b_0 = 0.0896 \text{ m m}^{-1}$ (or 9%) is the slope grade of the standard USLE plot, and m and n are respectively for the slope length factor L and the slope steepness factor S and vary according to the topographic conditions. The coefficients m and n were set to 0.6 and 1.3 respectively (Moore et al., 1993) and correspond closely to values reported in other studies for similar topographies (Moore and Burch, 1986; Renard et al., 1997; Nefeslioglu et al., 2008; Pike et al., 2009; Conforti et al., 2011; Luca et al., 2011). In this specific case study, A_s is given by the ratio of the upslope catchment area to grid size or, in other words, the product of contributing drainage area (in pixel) and grid size (e.g., Xu et al., 2008; Pike et al., 2009; Terranova et al., 2009; Conforti et al., 2011; Luca et al., 2011; Bosco et al., 2014). Assuming the flow width is invariant and equal to the grid size is generally the best approach in most practical circumstances (Chirico et al., 2005). Similarly to the USLE and the revised universal soil loss equation (RUSLE) models where a maximum length of slope has to be considered (Wischmeier and Smith, 1978; Renard et al., 1997; Bosco et al., 2014), we set a maximum value of flow accumulation equal to 10 pixels. This value corresponds to an accumulated slope length of 200 m, which falls within the range of most measured slope lengths (McCool et al., 1997).

In order to accommodate to more complex slopes, two other approaches were applied to compute the slope steepness factor S . The approach of McCool et al. (1987) uses two functions: one for slopes <9% and another for slopes >9% to compute the factor (S_{Mc}):

$$S_{Mc} = 10.8 \sin\theta + 0.03 \quad \text{when slope} < 9\% \quad (2)$$

$$S_{Mc} = 16.8 \sin\theta - 0.50 \quad \text{when slope} \geq 9\% \quad (3)$$

The approach of Nearing (1997) for computing S is based on a single function representative of all the slopes and that, in addition to McCool et al. (1987), is better at allowing for slopes greater than 22% to be considered. The resultant logistic equation to compute the factor (S_N) is given by:

$$S_N = -1.5 + 17/[1 + \exp(2.3 - 6.1 \sin\theta)] \quad (4)$$

TCI values were therefore derived by replacing S in Eq. (1) by Eqs. (2)–(4): TCI_{Mc} and TCI_N .

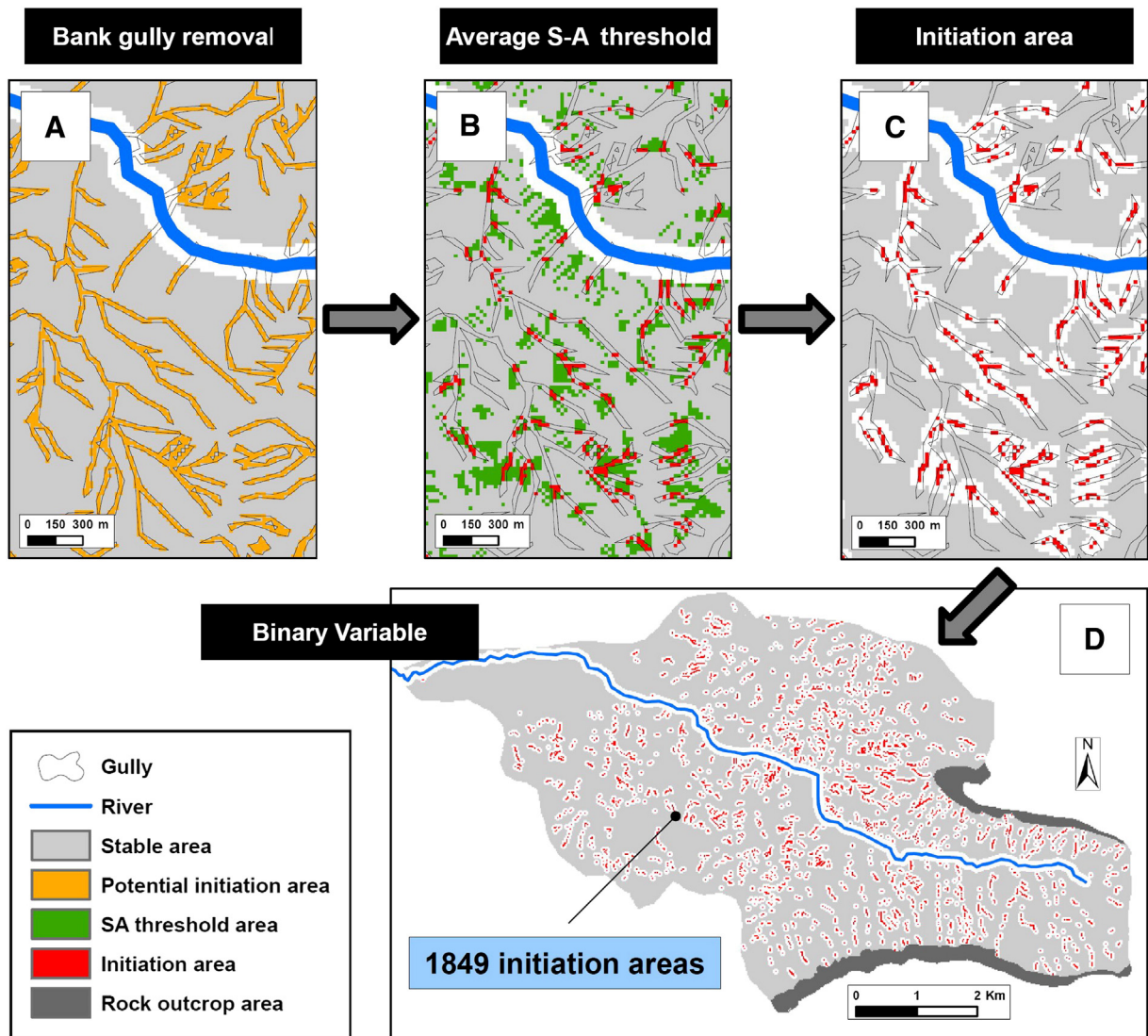


Fig. 3. Steps to extract the initiation areas (in red) of the existing gully network and to construct the binary variable (presence and absence of initiation) from which the dependent variable used in the modelling is derived. The stable area (in light grey) represents the places where no gully initiation associated with the existing gully network occurred. (A) Every gully is a potential initiation area (in orange) since the initiation areas have to lie within the mapped gully network. (B) S–A threshold areas (in green) are places where the thresholds are reached outside the mapped gullies within the stable areas. Initiation areas (in red) are places where the thresholds are reached within the gully network. (C) Each initiation is delimited by a 2-pixel uncertainty buffer area (in white). (D) The binary variable shows 1849 initiation areas (presence) and a stable area (absence). The rock outcrop areas (dark grey) are not part of the binary variable.

TWI reflects the tendency of water to accumulate at any point in the catchment and the tendency of gravitational forces to move that water downslope (Moore et al., 1991; Quinn et al., 1991). It has been used for characterizing the spatial distribution of zones of surface saturation and soil water content in a landscape (Daba et al., 2003; Lesschen et al., 2007; Nefeslioglu et al., 2008; Pike et al., 2009; Hancock and Evans, 2010; Conforti et al., 2011; Luca et al., 2011; Conoscenti et al., 2013). *TWI* can be expressed as:

$$TWI = \ln (A_s / \tan \theta) \quad (5)$$

SPI is directly proportional to stream power and it is a measure of the erosive power of overland flow (Moore et al., 1991). *SPI* is frequently used for estimating soil erosion by water (e.g., Daba et al., 2003; Nefeslioglu et al., 2008; Kakembo et al., 2009; Pike et al., 2009; Akgün and Türk, 2011; Conforti et al., 2011; Luca et al., 2011; Conoscenti et al., 2013) and is expressed as:

$$SPI = A_s \tan \theta \quad (6)$$

DTM resolution has an impact on the accuracy of the predictors (Quinn et al., 1991; Luca et al., 2011). For instance, it affects slope angle accuracy especially in areas of steep elevation changes and can cause a systematic underestimation of the slope gradient (Chang and Tsai, 1991; Florinsky, 1998). In addition, intrinsic errors related to the DTM can also impact the reliability of the predictors. The errors are mainly due to the inherent inaccuracy of the topographic map, the digitalization of the contour intervals, and the interpolation of the grid (Dewitte et al., 2008). Although their relative impact is difficult to quantify since we have no additional reference topographic material, it can be more or less important according to the type of variable considered. For instance, regarding “elevation” the relative impact is negligible in this specific region since it would be an error of a few tens of metres maximum for a local relief of several hundreds of metres. On the other hand, for the variables directly derived from the DTM, the impact could be more significant, especially where the topographic surface is less steep (Chang and Tsai, 1991; Florinsky, 1998). Among the primary topographic attributes, contributing drainage area should be the most sensitive to these errors. A small error in elevation can modify the direction of the flow path and hence its accumulation (Quinn et al., 1991). If it

happens in the upslope part of the watershed, close to the drainage divide where the accumulation values are small, such a modification should be very limited. On the other hand, the accumulations are larger downslope, and a modification in the flow direction can give a pixel a value far from the reality. Along the scarp line of a gully, the variability of flow accumulation can be very important from one pixel to another. However, if we assume that the DTM errors are randomly distributed, no trend should appear. The errors along the gully systems should concern only small groups of pixels randomly spread out and independent from each other. Actually, the impact of the errors on the real pattern of flow accumulation, and to a lesser extent on the other primary topographic attributes, should be very limited. It has however to be considered in the evaluation criteria of the model and in their geomorphological significance.

In addition to the topographic derivatives, lithology is also a potential predictor variable. Even though the study area is in a quite homogeneous lithological context, it is expected that this parameter can help in understanding the spatial occurrence of gully initiation. This predictor is composed of four classes directly derived from the lithological map: marls, calcareous marls, marls and limestones, and alluvial deposits (Fig. 2).

Land use and land cover conditions are probably of primary importance for the initiation of the gullies in this region (Vandekerckhove et al., 2000; Nyssen et al., 2002, 2006; Lesschen et al., 2007; Takken et al., 2008; Frankl et al., 2011). However, as we do not know the age of the gullies, such analysis is problematic. Furthermore, the information that needs to be collected to infer about historical vegetation conditions usually requires an in-depth investigation, which is in contradiction with this research objective that is to use readily available common spatial information. Therefore information on vegetation cover will not be considered in the prediction model. In a similar way, the spatial variability of soil characteristics whose very local variation might be one of the key factors for explaining gully initiation and dynamics (Vandekerckhove et al., 2000; Istanbuluoglu et al., 2005), is not considered either because such data are unavailable.

3. Reconstruction of the gully initiation areas

3.1. Determining the S – A thresholds from the literature

The present approach is based on the consideration that the use of published data of S – A thresholds is a valid and useful concept to reconstruct the original area of gully initiation. However, the reliability of some measurements may be questioned. Ideally, topographic thresholds should be measured at the gully initiation point (Vandekerckhove et al., 2000; Nachtergaele et al., 2001; Vanwallegem et al., 2003). However, in the literature, the distinction between the S – A threshold at the gully head and that at the gully initiation point is often unclear. Although the initiation point remains the same over a gully's lifetime, the gully head does change, unless we speak of gullies that grow not by regressive but by forward erosion. This can give different values as, for instance, A is shrinking with the upslope migration of the gully (Nyssen et al., 2002). In addition, the methodology used to assess S and A also affects the topographic thresholds. For example, local S derived from topographic maps usually underestimates local S measured in the field (Poesen et al., 2002, 2003). The threshold values can also vary according to the resolution of the DTM (Hancock and Evans, 2006; Nazari Samani et al., 2009; Millares et al., 2012). We therefore aim to obtain average thresholds in order to reduce the potential effect of the inherent uncertainty linked to the published values.

Since the topographic thresholds can vary with lithology, soil characteristics, vegetation and land use, climate and fire regime (Montgomery and Dietrich, 1988, 1994; Prosser and Slade, 1994; Vandekerckhove et al., 2000; Poesen et al., 2002; Hyde et al., 2007; Hancock and Evans, 2010), our aim is to obtain average values representative of the study area and the assumed general conditions that lead to

gully initiation. We focused our attention only on thresholds measured for permanent gullies since measurements at the gully heads indicate that the topographical thresholds for permanent gully formation are significantly higher compared to ephemeral gully formation (Poesen et al., 2003; Vanwallegem et al., 2005b). To consider thresholds that correspond to the climatic conditions that prevailed when the gullies initiated, we relied on the assumptions made in Section 2.1 and considered values that were measured in arid, semi-arid and Mediterranean environments (Table 2). For each region presented in Table 2, we considered the maximum and the minimum values of the dataset for both the slope gradient and the drainage area thresholds.

The thresholds can vary if the channel initiation is due to overland flow or landsliding (Montgomery and Dietrich, 1994). It is usually found that channels that initiate when the critical slope gradient value is higher than 0.5 m m^{-1} are usually associated with mass movement processes, whereas incision by overland flow is dominant in more gentle areas (Montgomery and Dietrich, 1988, 1989, 1994; Prosser and Abernethy, 1996; Vandekerckhove et al., 2000; Zucca et al., 2006; Nazari Samani et al., 2009). Since we focused on gullies triggered by water, we did not consider threshold values of the gullies having a critical slope gradient higher than 0.5 m m^{-1} . The maximum and the minimum values of the threshold datasets of each region presented in Table 2 were therefore adjusted accordingly. Hence, the values for the critical slope that we consider in this study are decreased to a maximum of 0.5 m m^{-1} when they are initially above (See column “max*” in Table 2). In some regions, the gullies with the critical slope value above 0.5 m m^{-1} correspond to the smaller drainage areas (Montgomery and Dietrich, 1988, 1989). In this case, the non-consideration of the thresholds of these gullies implies the adjustment of the minimum drainage values towards a higher limit (See column “min***” in Table 2).

The average thresholds were calculated from the values in Table 2. It suggests that the actual gullies initiated in areas where critical topographic slope angles of the soil surface range from 6° to 25° and where the drainage areas extend from 0.21 to 3.54 ha. Threshold lines for gully development can be represented by a power-type equation (Vandaele et al., 1996; Poesen et al., 2011): $S = aA^b$ with a and b coefficients depending on the environmental characteristics. It could be possible to compute such a threshold line for the present study by averaging the coefficients computed for the various regions presented in Table 2. However, such an approach would not have permitted to consider the landslide issue and to adjust the thresholds accordingly.

3.2. Use of the S – A thresholds to locate the gully initiation areas

The reconstructed gully initiation areas have to be in the actual gully network that was mapped from the aerial photographs. In addition, they have to fall within the range of the average S – A thresholds determined from the literature (Table 2). Once the initiation areas are extracted, additional processing is needed for the susceptibility analysis (Fig. 1). The aim is to construct a binary variable (i.e. presence or absence) that locates the places where the existing gullies initiated (i.e. “initiation area”) or the places where they did not initiate (i.e. “stable area”). The dependent variable used for the LR modelling will be derived from the binary variable.

The binary variable was extracted in four steps (Fig. 3):

- (A) Removal of the area potentially most affected by bank gullyng;
- (B) Application of the average S – A thresholds extracted from literature (Table 2);
- (C) Consideration of a buffer of uncertainty around each initiation area;
- (D) Removal of the rock outcrop areas.

The river banks are the area potentially most affected by bank gullyng. From the interpretation of the aerial photographs it was not feasible to identify bank gullies from others. To reduce the possibility of considering this process in the analysis, a 100 m buffer zone along the river

Table 2

Threshold values of critical slope gradient of soil surface (S) and drainage area (A) inferred for permanent gully development (initiation) in a range of arid and semi-arid environments with Mediterranean characteristics. The values are taken from the literature. For each region we take the minimum and maximum values of the dataset. The values in bold in columns “max*” and “min**” correspond to adjusted values to consider slope gradients not higher than 0.5 m m^{-1} . Underlined numbers are the average values considered for this study.

Region	Land use	Slope gradient (m m^{-1})			Drainage area (ha)			Reference
		min	max	max*	min	min**	max	
Southern Sierra Nevada, California	Open oak woodland and grassland	0.15	0.7	0.5	0.6	0.9	8	Montgomery and Dietrich, 1988
Tennessee Valley, San Francisco, California	Grassland and coastal prairie	0.17	0.9	0.5	0.12	0.4	4	Montgomery and Dietrich, 1988, 1989
Stanford Hills, San Francisco, California	Open oak woodland and grassland	0.2	0.35	0.35	0.4	0.4	2.5	Montgomery and Dietrich, 1994
Northern Humboldt Range, Nevada	Rangeland	0.1	0.4	0.4	0.04	0.04	1.5	Montgomery and Dietrich, 1994
Gungoandra catchment, New South Wales, Australia	Pasture with sparse vegetation	0.04	0.7	0.5	0.3	0.3	3	Prosser and Abernethy, 1996
Sierra de Gata, Almeria, SE Spain	Rangeland	0.08	0.5	0.5	0.02	0.02	3	Vandekerckhove et al., 2000
Alentejo, S Portugal	Cropland and rangeland	0.06	0.5	0.5	0.02	0.02	0.9	Vandekerckhove et al., 2000
Lesvos island, Greece	Rangeland	0.25	0.75	0.5	0.007	0.007	1.5	Vandekerckhove et al., 2000
Central-Eastern Sardinia, Italy	Pasture	0.05	1.1	0.5	0.02	0.02	2	Zucca et al., 2006
Boushehr-Samal watershed, Southwestern Iran	Rangeland	0.01	0.7	0.5	0.003	0.003	9	Nazari Samani et al., 2009
Average		0.111	0.66	0.475	0.153	<u>0.211</u>	<u>3.54</u>	
Average slope angle (degrees)		<u>6</u>	33	<u>25</u>				

* Upper slope gradient limit is decreased to 0.5 m m^{-1} where landslides are reported.

** Minimum drainage area values adjusted according to the decreasing to 0.5 m m^{-1} of slope gradient values.

was removed from the study area (Fig. 3A). The buffer zone was estimated from the aerial photographs. The average S – A thresholds from Table 2 were then applied to the remaining watershed topography. Only the areas where the thresholds are reached within the actual gully network are considered as initiation areas (Fig. 3B).

As a result of the inaccuracy related to the topographic predictors, the grid resolution, and the delineation of the gullies from the aerial photographs, we cannot assure that a pixel located in a “stable area” just next to an “initiation area” is strictly associated with a place that did not undergo erosion during the initiation phase. Therefore, a buffer area of 2 pixels (i.e. 40 m) was defined around all the initiation places (Fig. 3C). This buffer is not considered as a part of the binary variable. Several initiation areas can extend along a gully; the other parts of the gully being part of the buffers and the stable area.

In total, 1849 initiation areas were extracted (Fig. 3D). Their size varies from 1 to 28 pixels; 56% of the areas having only one pixel. Their spatial distribution along the gullies is consistent with the geomorphological hypotheses made in Section 2.1. There is at least one initiation area for each gully system and their position is in agreement with the hypothesis of a regressive gully (Fig. 3C). When several initiations appear along a gully system, it also confirms the hypothesis that some channels may be the result of several independent initiations connected to each other while extending (e.g., Pederson et al., 2006). Logically, there is no initiation area along the ridgetops delimiting the watershed, where drainage area is small and topography is most prone to diffuse flow (Dietrich et al., 1992, 1993).

In the steepest areas of the watershed, along the north-east and south-east ridges (Fig. 2A), where initiation areas are missing, slope angles are frequently higher than 40° . From the aerial photographs and Google Earth images, the stratigraphy of the Eocene calcareous marls is clearly identifiable in these steep terrains, attesting the absence or the very poor development of soil. In these areas of rock outcrop, soil erosion linked to the development of a gully is therefore very limited or even impossible. For this reason, these outcrops were not considered as being part of the binary variable (Fig. 3D). The binary variable is therefore smaller in extent than the initial watershed, the rock outcrops being removed from the stable (non-initiation) area. The rock outcrop areas were nevertheless kept as part of the study area for the computing of the predictor variables. The rock outcrops might indeed constitute upper parts of contributing drainage areas used for the location of gully initiation places. The 1849 initiation areas constitute the “presence” of the binary variable and represent 5% of its total extent, whereas the stable area constitutes the “absence” and represents the remaining 95%.

4. Susceptibility modelling

The initiation area map presented in Section 3.2 shows where the actual gully network could have started. Based on the S – A thresholds information alone, we could also try to predict the susceptibility to new gullies (Fig. 3B). However, because of the poor quality of the data and the absence of field measurements, we used published field knowledge with a data-driven modelling approach such as the LR (Fig. 1) instead.

Since lithology is the only parameter which is not derived from topographic data, there is a need to see how the approach is sensitive to this predictor. For this purpose, we must test LR calibrations with and without the consideration of lithology in the initial dataset of predictor variables. In addition, using the factors “contributing drainage area” and “slope gradient” straight away in LR models might be seen as a circular flaw as these two predictors were used to define the dependent variable (Fig. 1). Calibrations will also be performed omitting them. Overall, four different LR models will be calibrated using four different datasets of predictor variables (Table 3):

- Dataset 1 that gives “Model ALL”: the LR model is derived from a set of data that initially includes all the predictor variables;
- Dataset 2 that gives “Model ALL-Litho”: the LR model is derived from a set of data that initially includes all the predictor variables except “lithology”;
- Dataset 3 that gives “Model ALL-AS”: the LR model is derived from a set of data that initially includes all the predictor variables except “contributing drainage area” and “slope gradient”;
- Dataset 4 that gives “Model ALL-AS-Litho”: the LR model is derived from a set of data that initially includes all the predictor variables except “contributing drainage area”, “slope gradient” and “lithology”.

4.1. Logistic regression

Stepwise LR was adopted to find the best-fitting model describing the relationship between the dependent variable (Y) and a set of independent (predictor) continuous and categorical variables (x_1, x_2, \dots, x_n). The outcome, or dependent variable, is binary or dichotomous, coded as 0 or 1, representing, absence or presence of the gully initiation places, respectively. The result of the regression can be interpreted as the probability of one state of the dependent variable. For the probability of occurrence of gully initiation, given independent variables, the logistic response function can be written as (Hosmer and Lemeshow, 2000):

$$P(Y = 1) = \pi(x) = 1/[1 + \exp(-(\beta_0 + \beta_1 x_1 + \beta_2 x_2 + \dots + \beta_n x_n))] \quad (7)$$

Table 3
Results of the four logistic regression models for gully initiation susceptibility assessment. The table shows the coefficient calibrated for the predictor variables that significantly ($P < 0.05$) influence the spatial distributions of the gully initiations.

Predictor variable	Model ALL		Model ALL-Litho		Model ALL-AS		Model ALL-AS-Litho	
	Coefficient ($P < 0.05$)	Order of inclusion	Coefficient ($P < 0.05$)	Order of inclusion	Coefficient ($P < 0.05$)	Order of inclusion	Coefficient ($P < 0.05$)	Order of inclusion
Intercept	−2.905		−5.007		2.466		−0.130	3
Elevation	−0.005	3	−0.003	3	−0.006	3	−0.003	no
Slope gradient	0.226	2	0.204	2		no		
Slope aspect								
North (ref.)								6
East	0.706	11	0.815	8	0.698	10	0.794	5
South	0.662	10	0.932	7	0.638	11	0.897	4
West	0.931	8	1.012	4	0.898	5	0.970	9
Profile curvature	0.171	12	0.167	9	0.193	12	0.178	2
Planform curvature	−1.401	1	−1.409	1	−1.176	2	−1.196	no
Contributing drainage area	−0.025	6	−0.024	6		no		col
Sediment Transport Capacity Index (TCI_M) [*]		col		col		col		col
TCI_{Mc} [*]		col		col		col		1
TCI_N [*]		col		col	0.247	1	0.231	7
Stream Power Index (SPI)		col		col	−0.003	7	−0.003	8
Topographic Wetness Index (TWI)	0.829	5	0.777	5	0.205	9	0.201	no
Lithology				no				
Marls (ref.)								
Calcareous marls	−1.502	7			−1.457	6		
Marls and limestones	−1.096	4			−1.074	4		
Alluvial deposits	−1.127	9			−1.145	8		

Col = variables are not included in the logistic regression modelling as they are collinear with other predictor variables.

No = variable not included in the initial dataset from which the LR model is calibrated.

(ref.) = reference category of the dummy variable.

* TCI adapted from Moore and Burch (1986); McCool et al. (1987), and Nearing (1997). See Eqs. (1), (2), and (3).

where $\pi(x)$ is the probability of occurrence, or susceptibility, of gully initiation, β_0 is the intercept, and β_i is the coefficient for the independent variable x_i . To fit the LR model in Eq. (7), the values of β_0 and β_i , the unknown parameters, are estimated by the maximum likelihood method. The output probability values range from 0 to 1, with 0 indicating a 0% of chance of gully initiation and 1 indicating a 100% probability. In order to model $\pi(x)$, Eq. (7) is linearized with the logit transformation. The logit, or logarithm of the odds (i.e. the probability of “gully initiation” divided by the probability of “non-initiation”), is linear in its parameters:

$$\log(\pi(x)/1-\pi(x)) = \beta_0 + \beta_1x_1 + \beta_2x_2 + \dots + \beta_nx_n \quad (8)$$

The dependent variable used in LR was directly derived from the binary variable computed in Section 3.2 (Fig. 3D). However, this binary variable needed some additional processing in order to ensure the best fitting performance of the model. Only one pixel was randomly selected for representing each initiation area in order to avoid possible spatial autocorrelation (Hosmer and Lemeshow, 2000; Diniz-Filho et al., 2003; Vanwalleghe et al., 2008); a cell adjacent to a (non-) initiation cell tending also to be (non-) initiation cell. The 1849 initiation pixels of the dependent variable represent 44% of the total area covered by the initiations. Moreover, an equal proportion of initiation cells and non-initiation cells was selected in order to avoid prevalence, i.e. a considerable difference between initiation-affected and initiation-free areas (Hosmer and Lemeshow, 2000; Dai et al., 2004; Begueria, 2006). Stratified random sampling of 1849 cells located in the stable area, i.e. outside the gully initiation areas (Fig. 3D) was therefore preformed.

As the validity of the model needs to be measured (Chung and Fabbri, 2003; Brus et al., 2011), the sample of 3698 cells (2×1849) was partitioned randomly into a calibration dataset containing 80% of the cells (2958 pixels, i.e. 1479 initiation pixels and 1479 non-initiation pixels) and a validation dataset containing the remaining 20% of the cells; which is a good trade-off with regard to the number of predictor variables (Fielding and Bell, 1997). The LR procedure was applied to the calibration dataset that represents 5% of the study area.

LR requires coding a categorical variable with m categories into a $m-1$ dichotomous dummy variables and an additional reference category (Table 3). In this case, the category that covers the larger spatial extent was used as the reference category for each categorical variable. After the coding of the categorical variables, a multicollinearity analysis was performed among the independent variables; a model fitted via LR being sensitive to the collinearities (Hosmer and Lemeshow, 2000). Using the SAS software, the variance inflation factor (VIF) and the tolerance (TOL) statistics produced by linear regression were used for the diagnostic. Variables with $VIF > 2$ and $TOL < 0.4$ were excluded from the logistic analysis (Allison, 2001; Van Den Eeckhaut et al., 2006). Then stepwise LR was applied in order to select the best predictor variables to explain the occurrence of gully initiation.

4.2. Fitting performance of the susceptibility models

The fitting performance and the uncertainty of the calibrated gully susceptibility models were estimated using standard methods: four-fold plots (e.g. Rossi et al., 2010), Receiver Operating Characteristic (ROC) curves (e.g. Begueria, 2006; Van Den Eeckhaut et al., 2006; Vanwalleghe et al., 2008; Gómez Gutiérrez et al., 2009b; Rossi et al., 2010; Akgün and Türk, 2011; Eustace et al., 2011; Märker et al., 2011), and success rate and prediction rate curves (e.g. Chung and Fabbri, 2003; Guzzetti et al., 2006; Dewitte et al., 2010; Luca et al., 2011; Conoscenti et al., 2013).

A four-fold plot is a visual representation of a confusion matrix that summarizes the number of true positives (TP), true negatives (TN), false positives (FP), and false negatives (FN). For our research, the decision probability threshold to classify a pixel as a initiation or non-initiation area is set at a typical value of 0.5 given the equal number of gully and non-gully initiation points in the calibration sample (Fielding and Bell, 1997).

The ROC curve allows the predictive power of a model to be assessed independently of a specific probability threshold (Fielding and Bell, 1997; Begueria, 2006). It plots all the combinations of “sensitivity” (y -axis) vs. $1 -$ “specificity” (x -axis) that are obtained for an

Table 4
Association between gully initiation and the predictor variables (significance level = 0.01). These tests are applied to the calibration dataset.

Predictor variable	χ^2	Cramer's V
Elevation	203.5	0.262
Slope gradient	949.3	0.567
Slope aspect	296.5	0.317
Profile curvature	436.8	0.384
Planform curvature	694.8	0.485
Contributing drainage area	1221.8	0.643
Sediment Transport Capacity Index (TCI_M) [*]	1335.9	0.672
TCI_{Mc} [*]	1386.7	0.685
TCI_{N} [*]	1305.1	0.664
Stream Power Index (SPI)	1275.1	0.657
Topographic Wetness Index (TWI)	838.1	0.532
Lithology	83.1	0.168

^{*} TCI adapted from Moore and Burch (1986); McCool et al. (1987), and Nearing (1997). See Eqs. (1), (2), and (3).

entire range of possible thresholds. The “sensitivity”, or true positive rate, is $TP/(TP + FN)$, and $1 -$ “specificity”, or false positive rate, is $1 - TN/(FP + TN)$, which is equivalent to $FP/(FP + TN)$. The “sensitivity” is the proportion of pixels containing known gully initiations that are correctly classified as susceptible, and “specificity” is the proportion of pixels free of initiation classified as initiation-free. The area under the ROC curve, abbreviated AUC , is a measure of discrimination that summarizes the information contained in a plot (Hosmer and Lemeshow, 2000). $AUC = 0.5$ means no discrimination or

random forecast, whereas $AUC = 1$ means perfect discrimination. The higher the curve above the diagonal line (i.e. $AUC = 0.5$), the better the model. In practice it is extremely unusual to observe AUC greater than 0.9 (Hosmer and Lemeshow, 2000).

Success rate and prediction rate curves are both obtained by varying the decision threshold and comparing the percentage of the total area of known initiations in each susceptibility class with the percentage area of the susceptibility class. The curves plot the cumulative percentage of gully initiation area in each susceptibility class (y -axis) against the respective portions of the study area ranked from most to least susceptible (x -axis). Success rate curves are constructed considering the gullies of the calibration dataset that was used for the susceptibility model, whereas prediction rate curves are determined on the gullies of the validation dataset. In this study, since we are using an equal proportion of gully pixels and gully-free pixels, the success rate and prediction rate curves are, like the ROC curves, not sensitive to prevalence.

To further investigate the reliability of the susceptibility assessments obtained with the calibration dataset, the estimates for the model errors in each pixel were obtained adopting a “bootstrapping” re-sampling technique using the same gully initiation and thematic information but selecting a reduced number of pixels (Guzzetti et al., 2006; Kuhnert et al., 2010; Rossi et al., 2010). An ensemble of 200 susceptibility calibration runs was performed, each time using 2366 pixels (1183 gully and 1183 non-gully) randomly selected, corresponding to 80% of the total number of grid cells of the calibration dataset. The mean (μ) and the standard deviation (σ) for the probability (susceptibility) estimates of each pixel were obtained from the 200 model runs. These

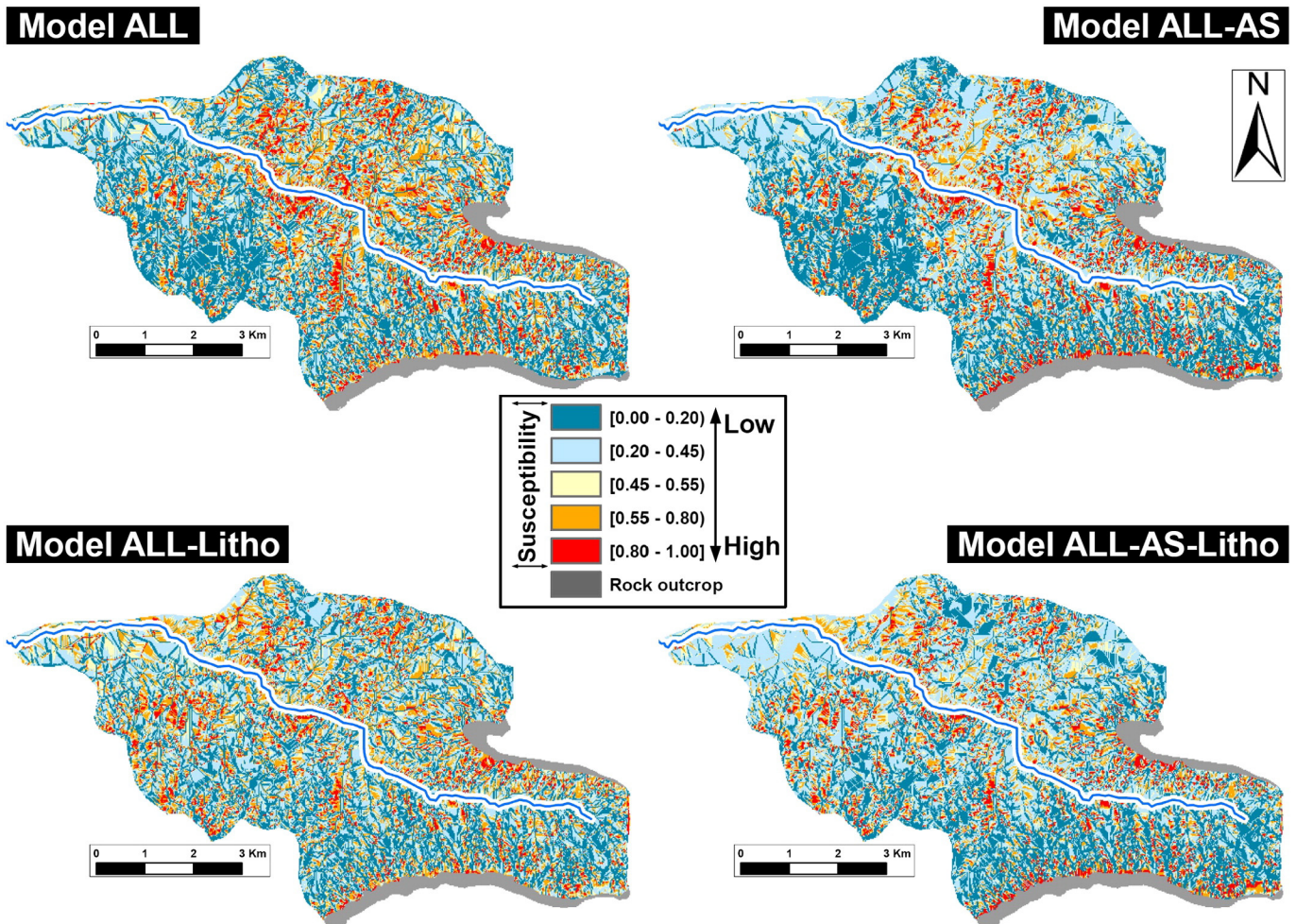
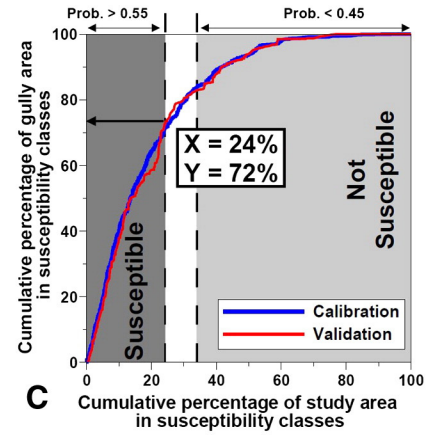
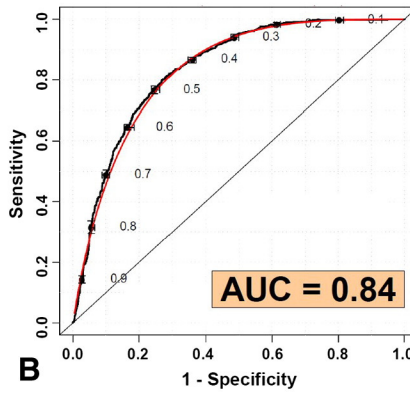
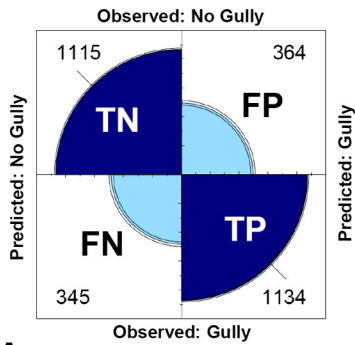


Fig. 4. Susceptibility maps portraying the four gully initiation models presented in Table 3.

Model ALL

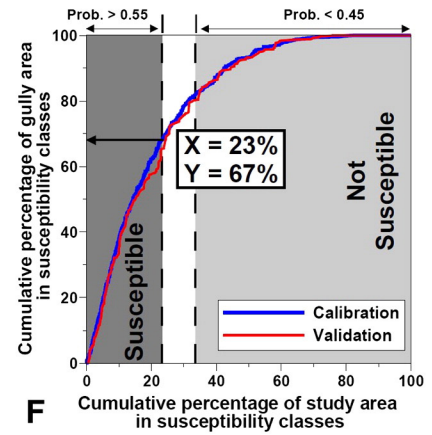
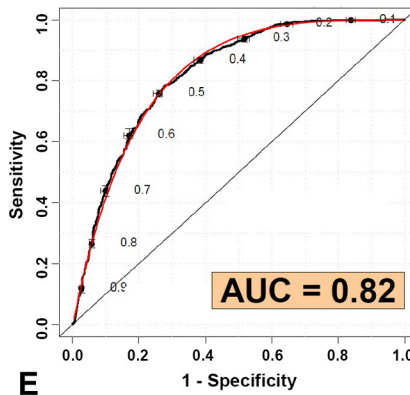
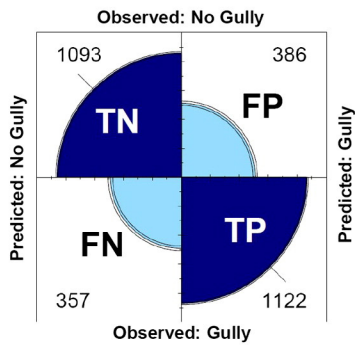


A

B

C

Model ALL-Litho

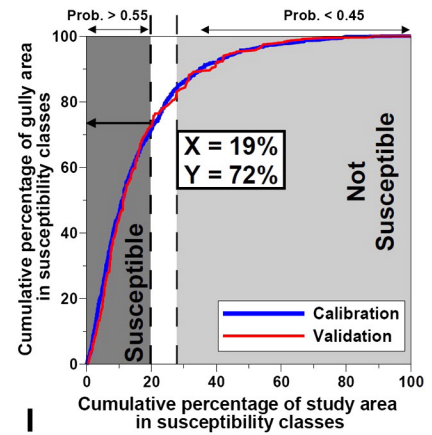
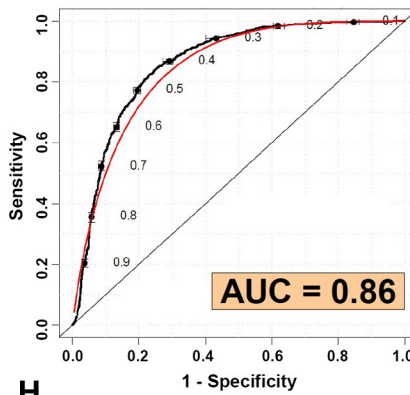
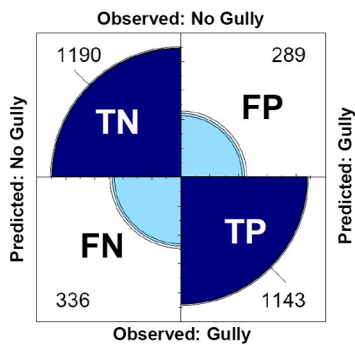


D

E

F

Model ALL-AS

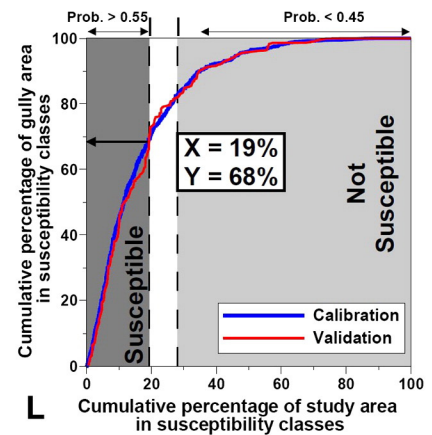
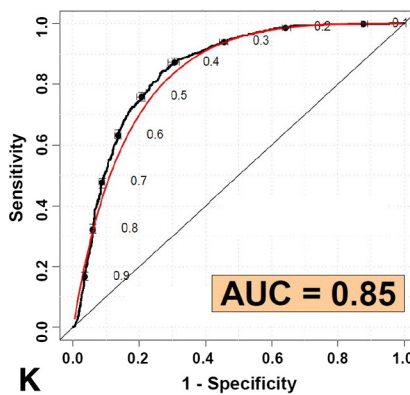
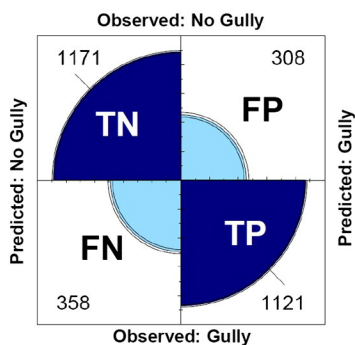


G

H

I

Model ALL-AS-Litho



J

K

L

statistics are shown in a graph where the two standard deviations (2σ) of the susceptibility estimate (y -axis) are plotted against their mean value (μ) (x -axis) (Guzzetti et al., 2006; Rossi et al., 2010).

The stepwise LR analysis was performed with SAS software and the fitting performance analyses were conducted using the open-source data analysis environment R (R Development Core Team, 2010) with several packages as well as the script written by Rossi et al. (2010).

5. Results and discussion of the susceptibility modelling

5.1. Combinations of predictor variables and susceptibility scenarios

To support the selection of the four datasets (Table 3), Chi-square (χ^2) statistics were first applied to confirm the suggested association between each predictor variable and the occurrence of gully initiation (e.g. Van Den Eckhaut et al., 2006; Geissen et al., 2007; Dewitte et al., 2010). The Cramer's V statistics, based on the χ^2 values, were then applied to test the strength and the type of association (Bonham-Carter, 1994). χ^2 values correspond to an absolute measure of the association and are useless in themselves, while the V index gives a standardized value ranging between 0 and 1. The closer V is to 1, the stronger is the association between the two variables (e.g., Achten et al., 2008; Dewitte et al., 2010). The χ^2 and Cramer's V statistics show that all the predictor variables collected for the analysis are associated with gully initiation, confirming significant difference between the distribution of values for the cells affected by gully initiation and that for the stable cells (Table 4). Potentially, all the predictor variables can be used for the modelling; "TCI", "SPP", "contributing drainage area" and "slope gradient" having, in this case, the highest predictive power.

The multicollinearity analysis was applied to the four datasets (Table 3). It revealed that for Model ALL and Model ALL-Litho the three TCI indices together with SPI had to be excluded from the LR analysis to reduce multicollinearity. For Model ALL-AS and Model ALL-AS-Litho, the multicollinearity analysis revealed that among the three TCI indices, the one derived from Nearing's equation TCI_N (Nearing, 1997) is the more suitable for this specific case. Even though it was expected that only one of the three TCI has to be used to avoid multicollinearity, the analysis highlights the index that considers more complex topographic conditions.

Except for the predictor variables excluded with the multicollinearity analysis, the LR functions did select all the remaining environmental variables of each dataset as the combination of predictors for the presence or absence of gully initiation in each grid cell (Table 3). The main difference between the four evaluations is therefore due to the pre-selection of the variables that were inserted in the datasets. The presence or absence of lithology has no impact on the multicollinearity and limited impact on the value of the coefficient, in agreement with the low Cramer's V value (Table 4). On the other hand, the exclusion of drainage area and slope gradient logically implies that the models are including the topographic indexes TCI_N , SPI and TWI . In the four assessments, it can be seen that, except for the intercepts, the sign of the coefficients remains the same for each predictor variable and only its value changes. This consistency could be interpreted as a result of the stability of the approach.

5.2. Susceptibility maps

Fig. 3 portrays the maps obtained for the four LR estimations in Table 3. The predicted gully susceptibility values are presented in five unequally spaced classes: [0.0–0.2]; [0.2–0.45]; [0.45–0.55]; [0.55–0.80]; and [0.80–1.0] (e.g., Guzzetti et al., 2006; Van Den Eckhaut et al.,

2009; Rossi et al., 2010). The two classes below 0.45 correspond to low susceptibility values, i.e. places that can be considered as stable. High susceptibility values are above 0.55 and are considered to be places prone to gully initiation. The intermediate value class [0.45–0.55] around the decision probability threshold value represents the undefined areas. The visual comparison of the four LR zonations reveals little differences in the proportion covered by the susceptibility classes showing very similar classification performances. Actually, ~10% of the pixels fall in the class with the highest susceptibility values [0.80–1.0] and ~60% of them correspond to low susceptibility values. The class corresponding to intermediate values [0.45–0.55] is of a limited extent, revealing a relatively good classification performance of the models.

The results shown in Fig. 4 were evaluated quantitatively with the four-fold plots, ROC curves, and success rate and prediction rate curves (Fig. 5). Considering the number of grid cells correctly classified by the four susceptibility models when the decision probability threshold is set at 0.5 (Fig. 4A,D,G,J), Model ALL-AS performed as the best. It classified correctly 79% (2333) of the total calibration sample as gully initiation ($TP = 1143$, 39%) or stable ($TN = 1190$, 40%). However the four-fold plots clearly shows that the predictive performance of the other models, even though being lower, are quite similar. Model ALL-AS-Litho (77%, 2292) performed better than Model All (76%, 2249) and Model All-Litho (75%, 2215).

The results shown by the ROC curves (Fig. 5B,E,H,K) lead to a similar conclusion. Model ALL-AS ($AUC = 0.86$) performs better, then Model ALL-AS-Litho, Model ALL and Model All-Litho ($AUC = 0.85$, 0.84 and 0.83 respectively) follow. These differences are very marginal and, as a general rule, $AUC = 0.8$ – 0.9 is considered excellent discrimination (Hosmer and Lemeshow, 2000).

The success rate and prediction rate curves of the four models are both very similar (Fig. 5C,F,I,L). At the probability threshold $p = 0.55$ that discriminates between susceptible and not susceptible areas, the prediction rates are around 70%. For Model ALL-AS, the prediction rate curve (red line) reveals that 72% of the area covered by gully initiation is located in the 19% most susceptible area. This measure of the model prediction skill shows also that Model ALL-AS performs the best.

Fig. 6 provides information on the uncertainty associated with the gully susceptibility models. The plots and the fitted curves show similarities and few differences. For the four classification models, the measure of variation, (2σ), is the lowest for pixels classified as having high susceptibility (probability ≥ 0.80) and low susceptibility (probability ≤ 0.20). It indicates that the classification models consistently identified these areas as prone to gully initiation or not. The scatter for the estimated errors becomes larger for the intermediate values of the susceptibility (between 0.45 and 0.55), suggesting not only that the models were less capable to classify these pixels as stable or unstable, but also that the obtained estimates are more variable, and hence, less reliable (Guzzetti et al., 2006; Van Den Eckhaut et al., 2009; Rossi et al., 2010). All the models are affected by a very similar uncertainty.

Based on the various quantitative evaluation criteria (Figs. 5 and 6), Model ALL-AS provides the best data combination to predict the spatial occurrence of gully initiation. However, the differences between the four models are very small, which is probably due to the fact that most of the information brought by the predictor variables is derived from the same data source, therefore providing a similar input.

5.3. Geomorphological significance of the predictions

The quantitative evaluation of the fitting performances of the models show that they all are reliable classifiers. In addition, the quite

Fig. 5. Fitting performances of the four gully initiation susceptibility models presented in Table 3. (A, D, G, J) Four-fold plots summarizing the number of true positives (TP), true negatives (TN), false positives (FP), and false negatives (FN). (B, E, H, K) Receiver Operating Characteristic (ROC) curves with various discrimination thresholds and the area under the ROC curve (AUC) value. In addition to the empirical ROC curve (black line), the binormal ROC curve (red line) is also fitted. The diagonal line $y = x$ represents the curve for a randomly constructed prediction. (C, F, I, L) Success rate and prediction rate curves derived from the calibration and validation datasets respectively. Dashed vertical lines indicate area percentage for susceptible (probability > 0.55) and non-susceptible (probability < 0.45) areas.

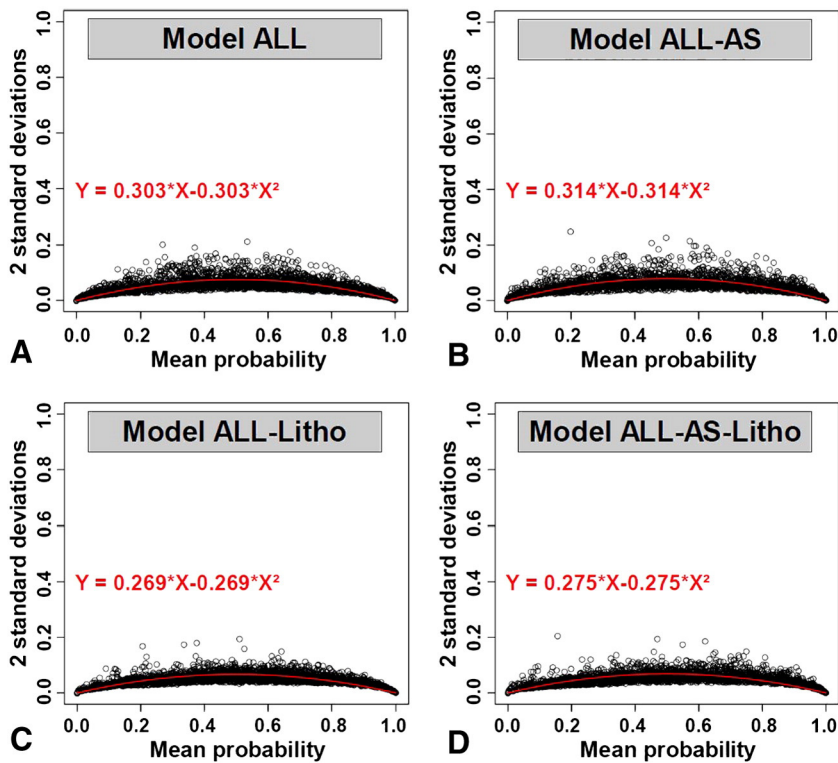


Fig. 6. Susceptibility model error. For the four susceptibility models, the plots show the mean value of 200 probability estimates for each pixel (black circle) against the two standard deviations (2σ) of the probability estimate. The red line shows the estimated model error obtained by regression fit (least square method).

similar modelling outputs attests the robustness of our approach. However, these quantitative estimates give no insight on how realistic they are (Fielding and Bell, 1997). There is therefore a need to invoke geomorphological criteria for better assessing the reliability of the models.

The first criterion is the spatial pattern of the areas of the highest susceptibility along the hillslopes and the gully channels; these areas being the places that are supposed to predict the occurrence of gully initiation places. Since the maps resulting from the models present few differences between each other (Fig. 4), the geomorphological discussion is solely based on the map given by Model ALL-AS (Fig. 7), because of its better fitting performance (Figs. 5 and 6). Fig. 7A reveals that the distribution of the susceptibility values and the areas of the highest probability are not uniformly and randomly distributed throughout the watershed. If the model had been efficient at predicting only the susceptibility to gully erosion without any distinction between the initiation places from the other parts of the channels, we could have expected that the high susceptibility areas would have shown a haphazard distribution throughout the watershed since gullies are developed on most slopes (Fig. 2). The observed pattern is a proof that the models allow only some part of the gullies to be discriminated; which in this case should correspond to the initiation areas.

Further inspection of the susceptibility map (Fig. 7B–D) allows us to highlight three characteristics of the processes linked to gully initiation. The first one is linked to the cases when one or several highly susceptible areas extend along the gullies. This is valid for both linear gullies and more complex systems (Fig. 7C,D). This pattern agrees with the hypothesis that some of these gullies can result from several initiations that developed independently at a series of knickpoints along the slope profile and connected to each other while migrating (e.g., Pederson et al., 2006).

Another pattern corresponds to places where areas of high susceptibility values concentrate. When it occurs within the central part (i.e. not at the border) of the watershed (see Fig. 7D for example), this corresponds to places of higher concentration of gullies. Note that these

gullies are generally shorter than the gullies that are assumed to have developed from several initiations (Fig. 7C). This difference can be that the former are developed closer to the small valley bottoms while the latter are developed on the slopes of the main valleys (i.e. the general slope lengths differs).

The third characteristic is identifiable at the ridges of the watershed, along the rock outcrops, where high susceptible areas also tend to concentrate (see Fig. 7B for example). These areas are places with higher slope gradients and where runoff from the rock outcrop areas can concentrate. They occur at the head of the gullies. Fig. 3D shows that several initiation areas are present a bit downslope of the rock outcrops. In this case we can assume that after their initiation, some of these gullies might have extended by downslope migration. Since rock outcrops should have a lower permeability than soil covered areas, we can imagine that drainage from these places is important for the contribution to water runoff that initiates the development of the channels.

Another criterion that needs to be pointed out is the geomorphological significance of the predictor variables that are in the data combinations (Dewitte et al., 2010). Although the best model, according to the quantitative criteria, is Model ALL-AS, we remain cautious in stating that one model is closer to the geomorphological reality than the other, especially with regard to the various assumptions and simplification of the landscape reality. In our approach we postulated that topography is sufficient to predict gully initiation. Without the consideration of potentially influencing variables like, for example, soil characteristics, vegetation cover, and human-induced landscape dynamic parameters (Vandekerckhove et al., 2000; Nyssen et al., 2002; Istanbuloglu et al., 2005; Nyssen et al., 2006; Lesschen et al., 2007; Takken et al., 2008; Gómez Gutiérrez et al., 2009a), this simple approach might result in prediction errors (Vandekerckhove et al., 1998). In addition, the models were not calibrated from data directly collected in the field.

Nevertheless, the modelling permits some geomorphological issues to be highlighted (Table 3). It confirms some of our hypotheses

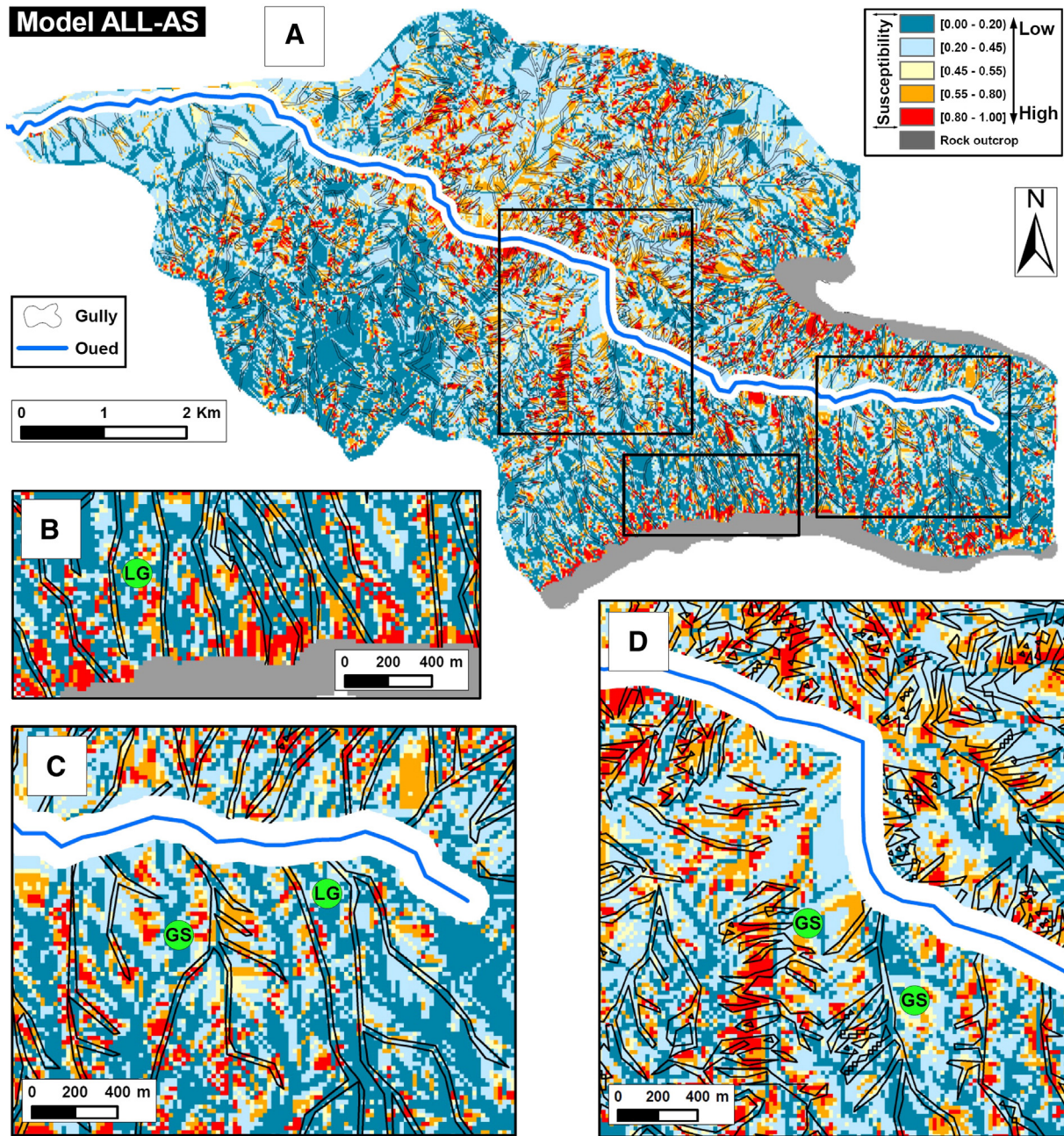


Fig. 7. Susceptibility maps portraying Model ALL-AS. Values closer to 1.0 show higher susceptibility to gully initiation. (B, C, D) Close-ups of gullies illustrating linear gullies (LG) and gully systems (GS).

concerning the processes behind the gully initiation as it highlights the importance of surface runoff and flow concentration through the integration of the predictors “planform curvature” and “Transport Capacity Index” (Table 3); these two predictors being the first to be included in the logistic regressions. The role of “slope gradient” is also confirmed as well as “elevation”. On the other hand, “slope aspect” is of smaller importance in this context.

In addition, as also pointed out by Prosser and Abernethy (1996), the simplification of our threshold approach assuming uniform vegetation and soil properties across the watershed does not mean that spatial variation in soil and vegetation is unrelated to the pattern of gully initiation susceptibility. The results merely imply that it is possible to constrain gully initiation by considering topography alone. It is known that variation in soils and vegetation can be influenced by topography and therefore can be partially implicitly modelled (e.g., Xu et al., 2008).

6. Conclusions

The development of a quantitative method for mapping the susceptibility to gully initiation in data-poor regions revealed the following insights:

- Using published *S–A* data with a low-data demanding statistical model like LR proves to be efficient when applied to common spatial data. The method provides relevant results in terms of statistical reliability and prediction performance.
- The use of average *S–A* information from the literature is an option when no field data are available. Such an approach establishes a methodology that allows similar studies to be undertaken elsewhere where there is a lack of data, especially in regions difficult to access. This could even have a potential application on Mars,

where gully erosion has already been the topic of numerous research (e.g., Mest et al., 2010).

- Despite data simplification, topographic threshold assumptions, and the non-consideration of soil characteristics, land use/cover conditions and human-induced landscape changes, the approach allows a better understanding of the gully processes in the region. It provides insights into factors controlling gully erosion and may allow the extrapolation and prediction of this erosion process in unsurveyed similar areas.
- The method provides information on the spatial pattern of the gully occurrence for the investigated region. The resulting susceptibility map is a useful tool for sustainable planning, conservation and protection of land from gully processes. Such a map could also be used by hydrological modellers interested in calculating sediment budgets.
- Topographic indices derived from common spatial data are shown to have the potential to be used for the location of gully initiation. This might show new ways for predicting soil erosion by water at regional scale since, so far, most erosion models do not predict the location of gullies (Jetten et al., 2003; Poesen et al., 2011).

Our approach is based almost exclusively on topographic data, and developed for permanent gullies in a specific Mediterranean semi-arid watershed. Therefore, the model cannot be expected to perform well in regions where land use (at the time of gully initiation) is highly variable and hydrological connectivity varies both spatially and temporally. The method, however, is worthy of applying to different climatic environments, and may not be restrictive to a specific type of gully. It could also be applied in a very similar way to ephemeral gullies.

Acknowledgements

Nel Caine, Irene Marzolf, Takashi Oguchi and two anonymous reviewers provided thoughtful reviews. Graham Sander is warmly thanked for his informal and friendly review of this manuscript.

References

- Achten, W.M.U., Dondeyne, S., Mugogo, S., Kafiriti, E., Poesen, J., Deckers, J., Muys, B., 2008. Gully erosion in South Eastern Tanzania: spatial distribution and topographic thresholds. *Z. Geomorphol.* 52, 225–235.
- Akgün, A., Türk, S., 2011. Mapping erosion susceptibility by a multivariate statistical method: A case study from the Ayvalik region, NW Turkey. *Comput. Geosci.* 37, 1515–1524.
- Allison, P.D., 2001. *Logistic regression using the SAS system: Theory and application*. Wiley Interscience, New York (288 pp.).
- Beguieria, S., 2006. Validation and evaluation of predictive models in hazard assessment and risk management. *Nat. Hazards* 37, 315–329.
- Bonham-Carter, G.F., 1994. *Geographic Information System for geoscientists: modelling with GIS*. Pergamon, New York.
- Bosco, C., de Rigo, D., Dijkstra, T., Sander, G., Wasowski, J., 2013. Multi-Scale robust modelling of landslide susceptibility – Regional rapid assessment and catchment robust fuzzy ensemble. *IFIP Adv. Inf. Commun. Technol.* 413, 321–335.
- Bosco, C., De Rigo, D., Dewitte, O., Poesen, J., Panagos, P., 2014. Modelling soil erosion at European scale: towards harmonization and reproducibility. *Nat. Hazards Earth Syst. Sci. Discuss.* 2, 2639–2680.
- Bou Kheir, R., Wilson, J., Deng, Y.X., 2007. Use of terrain variables for mapping gully erosion susceptibility in Lebanon. *Earth Surf. Process. Landf.* 32, 1170–1182.
- Brus, D.J., Kempen, B., Heuvelink, G.B.M., 2011. Sampling for validation of digital soil maps. *Eur. J. Soil Sci.* 62, 394–407.
- Bull, L.J., Kirkby, M.J., 1997. Gully processes and modelling. *Prog. Phys. Geogr.* 21, 354–374.
- Chang, K.T., Tsai, B.W., 1991. The effect of DEM resolution on slope and aspect mapping. *Cartogr. Geogr. Inf. Syst.* 18, 69–77.
- Chirico, G.B., Western, A.W., Grayson, R.B., Blöschl, G., 2005. On the definition of the flow width for calculating specific catchment area patterns from gridded elevation data. *Hydrol. Process.* 19, 2539–2556.
- Chung, C.F., Fabbri, A.G., 2003. Validation of spatial prediction models for landslide hazard mapping. *Nat. Hazards* 30, 451–472.
- Conforti, M., Aucelli, P.P.C., Robustelli, G., Scarciglia, F., 2011. Geomorphology and GIS analysis for mapping gully erosion susceptibility in the Turbolo stream catchment (Northern Calabria, Italy). *Nat. Hazards* 56, 881–898.
- Conoscenti, C., Agnesi, V., Angileri, S., Cappadonia, C., Rotigliano, E., Märker, M., 2013. A GIS-based approach for gully erosion susceptibility modelling: a test in Sicily, Italy. *Environ. Earth Sci.* 70, 1179–1195.
- Daba, S., Rieger, W., Strauss, P., 2003. Assessment of gully erosion in eastern Ethiopia using photogrammetric techniques. *Catena* 50, 273–291.
- Dai, F.C., Lee, C.F., Tham, L.G., Ng, K.C., Shum, W.L., 2004. Logistic regression modelling of storm-induced shallow landsliding in time and space of natural terrain of Lantau Island, Hong Kong. *Bull. Eng. Geol. Environ.* 63, 315–327.
- Daoudi, M., 2008. *Analyse et prédiction de l'érosion ravinante par une approche probabiliste sur des données multisources. Cas du bassin versant de l'Oued Isser, Algérie*. Unpublished PhD thesis, University of Liège, Liège, 287 pp.
- Desmet, P.J.J., Poesen, J., Govers, G., Vandaele, K., 1999. Importance of slope gradient and contributing area for optimal prediction of the initiation and trajectory of ephemeral gullies. *Catena* 37, 377–392.
- Dewitte, O., Jasselette, J.C., Cornet, Y., Van Den Eeckhaut, M., Collignon, A., Poesen, J., Demoulin, A., 2008. Tracking landslide displacements by multi-temporal DTMs: A combined aerial stereophotogrammetric and LIDAR approach in western Belgium. *Eng. Geol.* 99, 11–22.
- Dewitte, O., Chung, C.-J., Cornet, Y., Daoudi, M., Demoulin, A., 2010. Combining spatial data in landslide reactivation susceptibility mapping: A likelihood ratio-based approach in W Belgium. *Geomorphology* 122, 153–166.
- Dietrich, W.E., Wilson, C.J., Montgomery, D.R., McKean, J., Bauer, R., 1992. Erosion thresholds and land surface morphology. *Geology* 20, 675–679.
- Dietrich, W.E., Wilson, C.J., Montgomery, D.R., McKean, J., 1993. Analysis of erosion thresholds, channel networks, and landscape morphology using a digital terrain model. *J. Geol.* 101, 259–278.
- Diniz-Filho, J.A.F., Bini, L.M., Hawkins, B.A., 2003. Spatial autocorrelation and red herrings in geographical ecology. *Glob. Ecol. Biogeogr.* 12, 53–64.
- Dotterweich, M., Rodzik, J., Zgłobicki, W., Schmitt, A., Schmidtchen, G., Bork, H.-R., 2012. High resolution gully erosion and sedimentation processes, and land use changes since the Bronze Age and future trajectories in the Kazimierz Dolny area (Nałęczów Plateau, SE-Poland). *Catena* 95, 50–62.
- Eustace, A.H., Pringle, M.J., Denham, R.J., 2011. A risk map for gully locations in central Queensland, Australia. *Eur. J. Soil Sci.* 62, 431–441.
- Fielding, A.H., Bell, J.F., 1997. A review of methods for the assessment of prediction errors in conservation presence/absence models. *Environ. Conserv.* 24, 38–49.
- Florinsky, I.V., 1998. Accuracy of local topographic variables derived from digital elevation models. *Int. J. Geogr. Inf. Sci.* 12, 47–61.
- Frankl, A., Nyssen, J., De Dapper, M., Haile, M., Billi, P., Munro, R.N., Deckers, J., 2011. Linking long-term gully and river channel dynamics to environmental change using repeat photography (Northern Ethiopia). *Geomorphology* 129, 238–251.
- Geissen, V., Kampichler, C., Lopez-de Llergo-Juarez, J.J., Galindo-Acantara, A., 2007. Superficial and subterranean soil erosion in Tabasco, tropical Mexico: Development of a decision tree modeling approach. *Geoderma* 139, 277–287.
- Gómez Gutiérrez, A., Schnabel, S., Lavado Contador, J.F., 2009a. Gully erosion, land use and topographical thresholds during the last 60 years in a small rangeland catchment in SW Spain. *Land Degrad. Dev.* 20, 535–550.
- Gómez Gutiérrez, A., Schnabel, S., Felicísimo, Á.M., 2009b. Modelling the occurrence of gullies in rangelands of southwest Spain. *Earth Surf. Process. Landf.* 34, 1894–1902.
- Gómez Gutiérrez, A., Schnabel, S., Lavado Contador, J.F., 2009c. Using and comparing two nonparametric methods (CART and MARS) to model the potential distribution of gullies. *Ecol. Model.* 220, 3630–3637.
- Guns, M., Vanacker, V., 2012. Logistic regression applied to natural hazards: rare event logistic regression with replications. *Nat. Hazards Earth Syst. Sci.* 12, 1937–1947.
- Guzzetti, F., Reichenbach, P., Ardizzone, F., Cardinali, M., Galli, M., 2006. Estimating the quality of landslide susceptibility models. *Geomorphology* 81, 166–184.
- Hancock, G.R., Evans, K.G., 2006. Gully position, characteristics and geomorphic thresholds in an undisturbed catchment in northern Australia. *Hydrol. Process.* 20, 2935–2951.
- Hancock, G.R., Evans, K.G., 2010. Gully, channel and hillslope erosion – an assessment for a traditionally managed catchment. *Earth Surf. Process. Landf.* 35, 1468–1479.
- Hengl, T., 2006. Finding the right pixel size. *Comput. Geosci.* 32, 1283–1298.
- Hosmer, D.W., Lemeshow, S., 2000. *Applied logistic regression*. Wiley, New York.
- Hughes, A.O., Prosser, I.P., Stevenson, J., Scott, A., Lu, H., Gallant, J., Moran, C., 2001. Gully erosion mapping for the national land and water resources audit. CSIRO Land and Water Technical Report 26/01, CSIRO Land and Water, Canberra.
- Hyde, K., Woods, S.W., Donahue, J., 2007. Predicting gully rejuvenation after wildfire using remotely sensed burn severity data. *Geomorphology* 86, 496–511.
- Istanbulluoğlu, E., Tarboton, D.G., Pack, R.T., Luce, C., 2002. A probabilistic approach for channel initiation. *Water Resour. Res.* 38, 61–1–61–14.
- Istanbulluoğlu, E., Bras, R.L., Flores-Cervantes, H., Tucker, G.E., 2005. Implications of bank failures and fluvial erosion for gully development: Field observations and modeling. *J. Geophys. Res. F Earth Surf.* 110, F01014. <http://dx.doi.org/10.1029/2004JF000145>.
- Jetten, V., Govers, G., Hessel, R., 2003. Erosion models: Quality of spatial predictions. *Hydrol. Process.* 17, 887–900.
- Jetten, V., Poesen, J., Nachtergaele, J., van de Vlag, D., 2006. Spatial modelling of ephemeral gully incision: a combined empirical and physical approach. In: Owens, P.N., Collins, A.J. (Eds.), *Soil erosion and sediment redistribution in river catchments*. CAB International, Wallingford, UK, pp. 195–206.
- Kakembo, V., Xanga, W.W., Rowntree, K., 2009. Topographic thresholds in gully development on the hillslopes of communal areas in Ngqushwa Local Municipality, Eastern Cape, South Africa. *Geomorphology* 110, 188–194.
- Kirkby, M.J., Bull, L.J., Poesen, J., Nachtergaele, J., Vandekerckhove, L., 2003. Observed and modelled distributions of channel and gully heads – With examples from SE Spain and Belgium. *Catena* 50, 415–434.
- Kuhnert, P.M., Henderson, A.-K., Bartley, R., Herr, A., 2010. Incorporating uncertainty in gully erosion calculations using the random forests modelling approach. *Environmetrics* 21, 493–509.

- Lesschen, J.P., Kok, K., Verburg, P.H., Cammeraat, L.H., 2007. Identification of vulnerable areas for gully erosion under different scenarios of land abandonment in Southeast Spain. *Catena* 71, 110–121.
- Luca, F., Conforti, M., Robustelli, G., 2011. Comparison of GIS-based gully susceptibility mapping using bivariate and multivariate statistics: Northern Calabria, South Italy. *Geomorphology* 134, 297–308.
- Makanzu Imwangana, F., Dewitte, O., Ntombi, M., Moeyersons, J., 2014. Topographic and road control of mega-gullies in Kinshasa (DR Congo). *Geomorphology* 217, 131–139.
- Märker, M., Pelacani, S., Schroder, B., 2011. A functional entity approach to predict soil erosion processes in a small Plio-Pleistocene Mediterranean catchment in Northern Chianti, Italy. *Geomorphology* 125, 530–540.
- McCool, D.K., Brown, L.C., Foster, G.R., Mutchler, C.K., Meyer, L.D., 1987. Revised slope steepness factor for the Universal Soil Loss Equation. *Trans. ASAE* 30, 1387–1396.
- McCool, D.K., Foster, G.R., Weesies, G.A., 1997. Slope length and steepness factor (LS). In: Renard, K.G., Foster, G.R., Weesies, G.A., McCool, D.K., Yoder, D.C. (Eds.), *Predicting soil erosion by water: A guide to conservation planning with the revised universal soil loss equation (RUSLE)* Agriculture Handbook 703. United States Department of Agriculture (USDA), Agricultural Research Service, Washington, pp. 101–142 (384 pp.).
- Mest, S.C., Crown, D.A., Harbert, W., 2010. Watershed modeling in the Tyrrhena Terra region of Mars. *J. Geophys. Res. E Planets* 115, E09001. <http://dx.doi.org/10.1029/2009JE003429>.
- Meyer, A., Martinez-Casasnovas, J.A., 1999. Prediction of existing gully erosion in vineyard parcels of the NE Spain: a logistic modelling approach. *Soil Tillage Res.* 50, 319–331.
- Millares, A., Gulliver, Z., Polo, M.J., 2012. Scale effects on the estimation of erosion thresholds through a distributed and physically-based hydrological model. *Geomorphology* 153–154, 115–126.
- Montgomery, D.R., 1994. Road surface drainage, channel initiation, and slope instability. *Water Resour. Res.* 30, 1925–1932.
- Montgomery, D.R., Dietrich, W.E., 1988. Where do channels begin? *Nature* 336, 232–234.
- Montgomery, D.R., Dietrich, W.E., 1989. Source areas, drainage density, and channel initiation. *Water Resour. Res.* 25, 1907–1918.
- Montgomery, D.R., Dietrich, W.E., 1992. Channel initiation and the problem of landscape scale. *Science* 255, 826–830.
- Montgomery, D.R., Dietrich, W.E., 1994. Landscape dissection and drainage area-slope thresholds. In: Kirkby, M.J. (Ed.), *Process models and theoretical geomorphology*. Wiley, Chichester, pp. 221–246.
- Moore, I.D., Burch, G.J., 1986. Physical basis of the length-slope factor in the universal soil loss equation. *Soil Sci. Soc. Am. J.* 50, 1294–1298.
- Moore, I.D., Grayson, R.B., Ladson, A.R., 1991. Digital terrain modeling – a review of hydrological, geomorphological, and biological applications. *Hydrol. Process.* 5, 3–30.
- Moore, I.D., Gessler, P.E., Nielsen, G.A., Peterson, G.A., 1993. Soil attribute prediction using terrain analysis. *Soil Sci. Soc. Am. J.* 57, 443–452.
- Morgan, R.P.C., Mngomezulu, D., 2003. Threshold conditions for initiation of valley-side gullies in the Middle Veld of Swaziland. *Catena* 50, 401–414.
- Nachtergaele, J., Poesen, J., Steegen, A., Takken, I., Beuselinck, L., Vandekerckhove, L., Govers, G., 2001. The value of a physically based model versus an empirical approach in the prediction of ephemeral gully erosion for loess-derived soils. *Geomorphology* 40, 237–252.
- Nachtergaele, J., Poesen, J., Oostwoud Wijdenes, D., Vandekerckhove, L., 2002. Medium-term evolution of a gully developed in a loess-derived soil. *Geomorphology* 46, 223–239.
- Nazari Samani, A., Ahmadi, H., Jafari, M., Boggs, G., Ghoddousi, J., Malekian, A., 2009. Geomorphic threshold conditions for gully erosion in Southwestern Iran (Boushehr-Samal watershed). *J. Asian Earth Sci.* 35, 180–189.
- Ndomba, P.M., Mtaló, F., Killingtveit, A., 2009. Estimating gully erosion contribution to large catchment sediment yield rate in Tanzania. *Phys. Chem. Earth* 34, 741–748.
- Nearing, M.A., 1997. A single, continuous function for slope steepness influence on soil loss. *Soil Sci. Soc. Am. J.* 61, 917–919.
- Nefeslioglu, H.A., Duman, T.Y., Durmaz, S., 2008. Landslide susceptibility mapping for a part of tectonic Kelkit Valley (Eastern Black Sea region of Turkey). *Geomorphology* 94, 401–418.
- Nyssen, J., Poesen, J., Moeyersons, J., Luyten, E., Veyret-Picot, M., Deckers, J., Haile, M., Govers, G., 2002. Impact of road building on gully erosion risk: A case study from the Northern Ethiopian Highlands. *Earth Surf. Process. Landf.* 27, 1267–1283.
- Nyssen, J., Poesen, J., Veyret-Picot, M., Moeyersons, J., Haile, M., Deckers, J., Dewit, J., Naudts, J., Teka, K., Govers, G., 2006. Assessment of gully erosion rates through interviews and measurements: A case study from northern Ethiopia. *Earth Surf. Process. Landf.* 31, 167–185.
- Pederson, J.L., Petersen, P.A., Dierker, J.L., 2006. Gully erosion control at archaeological sites in Grand Canyon, Arizona. *Earth Surf. Process. Landf.* 31, 507–525.
- Pelletier, J.D., Quade, J., Goble, R.J., Aldenderfer, M.S., 2011. Widespread hillslope gully erosion on the southeastern Tibetan Plateau: Human or climate-change induced? *Geol. Soc. Am. Bull.* 123, 1926–1938.
- Perron, J.T., Kirchner, J.W., Dietrich, W.E., 2009. Formation of evenly spaced ridges and valleys. *Nature* 460, 502–505.
- Pike, A.C., Mueller, T.G., Schorgendorfer, A., Shearer, S.A., Karathanasis, A.D., 2009. Erosion index derived from terrain attributes using logistic regression and neural networks. *Agron. J.* 101, 1068–1079.
- Poesen, J., Vandekerckhove, L., Nachtergaele, J., Oostwoud Wijdenes, D., Verstraeten, G., van Wesemael, B., 2002. Gully erosion in dryland environments. In: Bull, L.J., Kirkby, M.J. (Eds.), *Dryland rivers: Hydrology and geomorphology of semi-arid channels*. Wiley, Chichester, UK, pp. 229–262.
- Poesen, J., Nachtergaele, J., Verstraeten, G., Valentin, C., 2003. Gully erosion and environmental change: importance and research needs. *Catena* 50, 91–133.
- Poesen, J.W.A., Torri, D.B., Vanwalleghem, T., 2011. Gully erosion: Procedures to adopt when modelling soil erosion in landscapes affected by gully erosion. In: Morgan, R.P.C., Nearing, M.A. (Eds.), *Handbook of erosion modelling*. John Wiley & Sons, Chichester, pp. 360–386.
- Prosser, I.P., Abernethy, B., 1996. Predicting the topographic limits to a gully network using a digital terrain model and process thresholds. *Water Resour. Res.* 32, 2289–2298.
- Prosser, I.P., Slade, C.J., 1994. Gully formation and the role of valley-floor vegetation, southeastern Australia. *Geology* 22, 1127–1130.
- Quinn, P., Beven, K., Chevallier, P., Planchon, O., 1991. The prediction of hillslope flow paths for distributed hydrological modelling using digital terrain models. *Hydrol. Process.* 5, 59–79.
- R Development Core Team, 2010. R: A language and environment for statistical computing, reference index version 2.11.1. R Foundation for Statistical Computing, Vienna, Austria 3-900051-07-0 ([URL http://www.R-project.org](http://www.R-project.org)).
- Renard, K.G., Foster, G.R., Weesies, G.A., McCool, D.K., Yoder, D.C., 1997. *Predicting soil erosion by water: A guide to conservation planning with the revised universal soil loss equation (RUSLE)*. Agriculture Handbook 703. United States Department of Agriculture (USDA), Agricultural Research Service, Washington (384 pp.).
- Rossi, M., Guzzetti, F., Reichenbach, P., Mondini, A.C., Peruccacci, S., 2010. Optimal landslide susceptibility zonation based on multiple forecasts. *Geomorphology* 114, 129–142.
- Rutherford, I.D., Prosser, I.P., Davis, J., 1997. Simple approaches to predicting rates and extent of gully development. In: Wang, S.S.Y., Langendoen, E.J., Shields Jr. (Eds.), *Proceedings of the conference on management of landscapes disturbed by channel incision*. Center for Computational Hydroscience and Engineering, University of Mississippi, USA, pp. 1125–1130.
- Seeger, M., Marzoff, I., Ries, J.B., 2009. Identification of gully-development processes in semi-arid NE-Spain. *Z. Geomorphol.* 53, 417–431.
- Shakesby, R.A., Doerr, S.H., 2006. Wildfire as a hydrological and geomorphological agent. *Earth Sci. Rev.* 74, 269–307.
- Sidorchuk, A., 1999. Dynamic and static models of gully erosion. *Catena* 37, 401–414.
- Svoray, T., Markovitch, H., 2009. Catchment scale analysis of the effect of topography, tillage direction and unpaved roads on ephemeral gully incision. *Earth Surf. Process. Landf.* 34, 1970–1984.
- Svoray, T., Michailov, E., Cohen, A., Rokah, L., Sturm, A., 2012. Predicting gully initiation: comparing data mining techniques, analytical hierarchy processes and the topographic threshold. *Earth Surf. Process. Landf.* 37, 607–619.
- Takken, I., Croke, J., Lane, P., 2008. Thresholds for channel initiation at road drain outlets. *Catena* 75, 257–267.
- Terranova, O., Antronico, L., Coscarelli, R., Iaquina, P., 2009. Soil erosion risk scenarios in the Mediterranean environment using RUSLE and GIS: An application model for Calabria (southern Italy). *Geomorphology* 12, 228–245.
- Touazi, M., Laborde, J.-P., Bhury, N., 2004. Modelling rainfall – discharge at a mean inter-yearly scale in northern Algeria. *J. Hydrol.* 296, 179–191.
- Touchan, R., Anchukaitis, K.J., Meko, D.M., Sabir, M., Attalah, S., Aloui, A., 2011. Spatiotemporal drought variability in northwestern Africa over the last nine centuries. *Clim. Dyn.* 37, 237–252.
- Van Den Eckhaut, M., Vanwalleghem, T., Poesen, J., Govers, G., Verstraeten, G., Vandekerckhove, L., 2006. Prediction of landslide susceptibility using rare events logistic regression: A case-study in the Flemish Ardennes (Belgium). *Geomorphology* 76, 392–410.
- Van Den Eckhaut, M., Reichenbach, P., Guzzetti, F., Rossi, M., Poesen, J., 2009. Combined landslide inventory and susceptibility assessment based on different mapping units: an example from the Flemish Ardennes, Belgium. *Nat. Hazards Earth Syst. Sci.* 9, 507–521.
- Vandaele, K., Poesen, J., Govers, G., Van Wesemael, B., 1996. Geomorphic threshold conditions for ephemeral gully incision. *Geomorphology* 16, 161–173.
- Vandekerckhove, L., Poesen, J., Oostwoud Wijdenes, D., De Figueiredo, T., 1998. Topographical thresholds for ephemeral gully initiation in intensively cultivated areas of the Mediterranean. *Catena* 33, 271–292.
- Vandekerckhove, L., Poesen, J., Oostwoud Wijdenes, D., Nachtergaele, J., Kosmas, C., Roxo, M.J., De Figueiredo, T., 2000. Thresholds for gully initiation and sedimentation in Mediterranean Europe. *Earth Surf. Process. Landf.* 25, 1201–1220.
- Vanwalleghem, T., Van Den Eckhaut, M., Poesen, J., Deckers, J., Nachtergaele, J., Van Oost, K., Slenters, C., 2003. Characteristics and controlling factors of old gullies under forest in a temperate humid climate: A case study from the Meerdaal Forest (Central Belgium). *Geomorphology* 56, 15–29.
- Vanwalleghem, T., Bork, H.R., Poesen, J., Schmidtchen, G., Dotterweich, M., Nachtergaele, J., Bork, H., Deckers, J., Bruschi, B., Bungeers, J., De Bie, A., 2005a. Rapid development and infilling of a buried gully under cropland, central Belgium. *Catena* 63, 221–243.
- Vanwalleghem, T., Poesen, J., Nachtergaele, J., Verstraeten, G., 2005b. Characteristics, controlling factors and importance of deep gullies under cropland on loess-derived soils. *Geomorphology* 69, 76–91.
- Vanwalleghem, T., Van Den Eckhaut, M., Poesen, J., Govers, G., Deckers, J., 2008. Spatial analysis of factors controlling the presence of closed depressions and gullies under forest: Application of rare event logistic regression. *Geomorphology* 95, 504–517.
- Wischmeier, W.H., Smith, D.D., 1978. *Predicting rainfall erosion losses: a guide to conservation planning*. Agriculture Handbook 537. United States Department of Agriculture (USDA), Agricultural Research Service, Washington (58 pp.).
- Xu, X.-L., Ma, K.-M., Fu, B.-J., Song, C.-J., Liu, W., 2008. Relationships between vegetation and soil and topography in a dry warm river valley, SW China. *Catena* 75, 138–145.
- Zucca, C., Canu, A., Della Peruta, R., 2006. Effects of land use and landscape on spatial distribution and morphological features of gullies in an agropastoral area in Sardinia (Italy). *Catena* 68, 87–95.